



HAL
open science

The genome of the blind bee louse fly reveals deep convergences with its social host and illuminates *Drosophila* origins

Héloïse Bastide, Hélène Legout, Noé Dogbo, David Ogereau, Carolina Prediger, Julie Carcaud, Jonathan Filée, Lionel Garnery, Clément Gilbert, Frédéric Marion-Poll, et al.

► To cite this version:

Héloïse Bastide, Hélène Legout, Noé Dogbo, David Ogereau, Carolina Prediger, et al.. The genome of the blind bee louse fly reveals deep convergences with its social host and illuminates *Drosophila* origins. *Current Biology - CB*, 2024, 10.1016/j.cub.2024.01.034 . hal-04452751

HAL Id: hal-04452751

<https://hal.science/hal-04452751>

Submitted on 12 Feb 2024

HAL is a multi-disciplinary open access archive for the deposit and dissemination of scientific research documents, whether they are published or not. The documents may come from teaching and research institutions in France or abroad, or from public or private research centers.

L'archive ouverte pluridisciplinaire **HAL**, est destinée au dépôt et à la diffusion de documents scientifiques de niveau recherche, publiés ou non, émanant des établissements d'enseignement et de recherche français ou étrangers, des laboratoires publics ou privés.

1 Report

2 **The genome of the blind bee louse fly reveals deep convergences with its social host**
3 **and illuminates *Drosophila* origins**

4
5 Héloïse Bastide^{1,*}, Hélène Legout¹, Noé Dogbo¹, David Ogereau¹, Carolina Prediger¹, Julie
6 Carcaud¹, Jonathan Filée¹, Lionel Garnery¹, Clément Gilbert¹, Frédéric Marion-Poll^{1,2},
7 Fabrice Requier¹, Jean-Christophe Sandoz¹, Amir Yassin¹

8
9 ¹Université Paris-Saclay, CNRS, IRD, UMR Évolution, Génomes, Comportement et
10 Écologie, 91198 Gif-sur-Yvette, France.

11 ²Université Paris-Saclay, AgroParisTech, 91123 Palaiseau Cedex, France

12
13 ***Lead contact:** Héloïse Bastide (heloise.bastide@universite-paris-saclay.fr)

14

15

16

17

18 **Summary**

19 Social insects nests harbor intruders known as inquilines,¹ which are usually related to
20 their host.^{2,3} However, distant non-social inquilines may also show convergences with
21 their hosts,^{4,5} though the underlying genomic changes remain unclear. We analyzed the
22 genome of the wingless and blind bee louse fly *Braula coeca*, an inquiline kleptoparasite
23 of the Western honey bee *Apis mellifera*.^{6,7} Using large phylogenomic data, we confirmed
24 recent accounts that the bee louse fly is a drosophilid,^{8,9} and showed that it had likely
25 evolved from a sap-breeder ancestor associated with honeydew and scale insects wax.
26 Unlike many parasites, the bee louse fly genome did not show significant erosion or strict
27 reliance on an endosymbiont, likely due to a relatively recent age of inquilinism. However,
28 we observed a horizontal transfer of a transposon and a striking parallel evolution in a
29 set of gene families between the honey bee and the bee louse fly. Convergences included
30 genes potentially involved in metabolism and immunity and the loss of nearly all bitter-
31 tasting gustatory receptors in agreement with life in a protective nest and a diet of honey,
32 pollen, and beeswax. Vision and odorant receptor genes also exhibited rapid losses. Only
33 genes whose orthologs in the closely related *Drosophila melanogaster* respond to honey
34 bee pheromones components or floral aroma were retained, whereas the losses included
35 orthologous receptors responsive to the anti-ovarian honey bee queen pheromones.
36 Hence, deep genomic convergences can underlie major phenotypic transitions during the
37 evolution of inquilinism between non-social parasites and their social hosts.

38

39 **Keywords:** parasitism; inquilinism; phylogenomics; horizontal transposon transfer; gene
40 family evolution; adaptation.

41 **Results and Discussion**

42 *The bee louse fly Braula coeca is an aberrant member of the Drosophilidae*

43 Among the several parasites and inquilines that are attracted by the rich resources
44 and clean and protective shelter of the Western honey bee *Apis mellifera* nest, none has
45 undergone as profound morphological changes as the apterous and quasi-blind bee louse
46 fly *Braula coeca* (Figure 1A-C). The female lays eggs in honey (not brood) cells, and the
47 hatched larvae eat pollen and wax, where they burrow tunnels in which they pupate
48 without forming true puparia.^{6,7} Following emergence, the adults attach to the body of
49 worker bees, migrating from one individual to another until reaching the queen (Figure
50 1A). There, they move to the queen's head, stimulate regurgitation, and imbibe from her
51 mouth honey and nectar.^{6,7} The bee louse fly is considered an inquiline kleptoparasite
52 with potential negative effects on honey bee colony health due to the galleries it makes in
53 bee combs and the facilitation of transmitting serious pathogenic viruses to the bees.¹⁰

54 Ever since Réaumur's first description of the bee louse fly in 1740, and Nitzsch's
55 creation of the genus *Braula* in 1818,^{11,12} the positioning within the Diptera of the bee
56 louse fly and affiliated species that were classified under the family Braulidae has been
57 puzzling because of its aberrant morphology and unique adaptations to a social host. This
58 family contains seven species belonging to the genera *Braula* and *Megabraula* that are all
59 inquilines to honey bee species of the genus *Apis*. Recent phylogenetic analyses based on
60 a transcriptome assembled from one adult fly and using 1,130 loci interestingly showed
61 *Braula coeca*, the most widespread braulid, to constitute a basal lineage within the
62 Drosophilidae that was sister to four genera of the subfamily Steganinae.^{8,9} To reassess
63 this hypothesis using a larger dataset, we sequenced the whole genome from a pooled
64 sample of 15 unsexed *B. coeca* flies, all collected on Ouessant Island in Western France.
65 We used a hybrid approach to assemble a genome using long-read Oxford Nanopore
66 Technology (ONT) and short-read Illumina sequencing (see Methods). Benchmarking
67 Universal Single-Copy Orthologs (BUSCO)¹³ gave a score of 95.8% of the Dipteran
68 conserved single-copy orthologs with 1.3% of duplicated genes. This value is higher than
69 the recommended score of 90% for reference genomes¹⁴. Merqury¹⁵ estimated an
70 assembly completeness of 93.6% and a consensus quality value (QV) of 41, which exceeds
71 the recommended threshold of QV40 for reference genome.¹⁶ We assembled two genomes
72 and one transcriptome of three additional steganine genera. We then built a supermatrix
73 of 3,100 BUSCO genes (2,557,349 amino acids) that included 15 drosophilid species

74 (representative members of the four main radiations in the family),¹⁷ and 5 species
75 belonging to the superfamily Ephydroidea to which both the Drosophilidae and Braulidae
76 belong (Table S1). The maximum-likelihood phylogenetic analysis of this large dataset
77 reconfirmed the close-relatedness of *B. coeca* to the Drosophilidae. It further showed that
78 it is a full member of the subfamily Steganinae (Figure 1D). The taxonomic priority
79 principle should consider the family Drosophilidae, described in 1856,¹⁸ a junior synonym
80 for the family Braulidae, described in 1853.¹⁹ However, the asymmetric size and scientific
81 relevance of the two families argue against such a decision. We, therefore, opt for
82 synonymizing the Braulidae with the Drosophilidae, referring hereafter to *Braula* and
83 *Megabraula* as members of the subfamily Steganinae.

84

85 *Inquilinism in the bee louse fly likely evolved from sap breeders associated with scale insects*

86 To gain further insight into the history of the association between *Braula* and *Apis*,
87 we mapped the predominant ecological habitats of ephydroid families on the phylogeny.
88 The ancestral habitat of ephydroids was presumed to be rotting leaf molds.²⁰ From this,
89 multiple specializations took place, including the exploitation of aquatic molds (and
90 eventually algae) in the Ephydriidae,²¹ Mammal dung in Curtonotidae and Diastatidae,^{21,22}
91 and fermenting vegetables and fruits, sap and fungi, with specialization mostly on yeasts
92 in the Drosophilidae²³ (Figure 1D). Bayesian reconstruction suggests the ancestral habitat
93 of the Drosophilidae to be tree sap breeding (Figure 1D) with fungus- and fruit-breeding
94 subsequently deriving and predominating in the genera *Leucophenga* and *Drosophila*,
95 respectively. Remarkably, the deepest branches in the Steganinae and the
96 Cryptochaetidae (the closest relative to the Drosophilidae) represent lineages whose
97 larvae are predatory of scale insects and mealy bugs, e.g., *Acletoxenus formosus* and *A.*
98 *indicus* on aleyrodoids, *Rhinoleucophenga brasiliensis* and *R. obesa* as well as
99 *Cryptochaetidum iceryae* and *C. grandicorne* on coccoids.²⁴ In those lineages, adults are
100 often seen to feed on the honeydew produced by the bugs, an abundant sugar-rich
101 substrate sucked from plants' sap, while larvae take shelter and develop in the waxy
102 secretions of these insects. This dependence on sugary substrate (honeydew) and
103 development in a waxy environment could have predisposed *Braula's* inquilinism in bee
104 nests.

105

106

107

108 *The bee louse fly inquilinism is relatively recent*

109 To date *Braula* inquilinism, we inferred a fossil-calibrated phylogeny using 79
110 single-copy orthologs (63,192 amino acids) in 17 Acalyptrate dipteran and 25 Apocrite
111 hymenopteran species (see Methods; Table S1; Figure 2A). Five non-ephydroid dipteran
112 species with Ref-Seq assemblies were included in this analysis to correct for tree
113 imbalance.²⁵ The divergence between *B. coeca* from its closest steganine relatives (node
114 1 in Figure 2A: 44.9 [37.8-53.8] million years (myr) [95% confidence interval])
115 overlapped with the origin of the Apidae (50.12 [42.9-64.5] myr) and with the transition
116 from solitary to subsocial (2: 40.25 [32.4-47.8] myr) and primitively social habits (3:
117 30.98 [26.3-36.0] myr).²⁶ It is possible that the origin of the bee louse fly-apid interactions
118 occurred at sap breeding sites, when early subsocial apids started to gather resin and
119 other plant exudates, as well as scale insects honeydew, and stored them in their nests. As
120 eusociality evolved (4: 23.8 [18.9-28.2] myr), the proportion of resin to secreted wax
121 diminished, and some cells were also used to store nectar and honey for the brood.²⁷ A
122 shift from the putatively ancestral dependence on honey and wax produced by scale
123 insects to those produced by bees might have evolved by then. The transition to
124 eusociality in the genus *Apis* required an important division of labor that involved the
125 evolution of pheromonal control of the reproductive capacity of worker females by the
126 queen and the evolution of trophallaxis.²⁷ Adaptation of *Braula* to the queen pheromone
127 compounds that have anti-ovarian effects on a wide range of insects, including *Drosophila*
128 *melanogaster*²⁸ and the exploitation of trophallaxis⁷ could not have evolved before the
129 advancement of eusociality (5: 17.1 [11.6-23.0] myr). The evolution of blindness and
130 apterism should have constrained the dispersal of the bee lice, relating their speciation
131 history to that of their hosts. Indeed, only seven bee louse fly species are known, of which
132 five *Braula* species are restricted to the Western honey bee *A. mellifera*, and two
133 *Megabraula* species are restricted to the giant honey bee *A. laboriosa* in the Himalayas.^{29,30}
134 The divergence between these *Apis* species, and presumably between *Braula* and
135 *Megabraula*, is estimated at 6: 5.8 [2.8 -12.0] myr ago. Therefore, the evolution of the bee
136 louse fly inquilinism has likely taken place during the Mid- to Late Miocene period
137 between 5.8 and 17.1 myr ago (Figure 2A). We cannot rule out even a more recent origin
138 if the ancestor of *Braula* or *Megabraula* has shifted from one *Apis* host to another, *i.e.* <5.8
139 myr ago.

140

141 *The bee louse fly inquilinism was accompanied by a reduction of gene content but not*
142 *genome size*

143 Loss of significant portions of genomic and gene contents is a characteristic of
144 obligate parasites specializing on specific hosts or inhabiting extreme environments. For
145 example, the human body louse, *Pediculus humanus*, has one of the smallest genomes and
146 the lowest numbers of genes in insects (108 megabases [Mb] and 10,773 protein-coding
147 genes).³¹ For *B. coeca*, we obtained a final assembly size of 309.35 Mb shared by 2,477
148 contigs with an N50 of 347,211 bp. This N50 estimate is typical of hybrid genome
149 assemblies obtained using a pooled sample of wild-caught drosophilid flies from species
150 with large genome sizes (> 300 Mb).³² No evidence for polyploidy or other endosymbiont
151 that could have biased the genome size estimate was detected (Figure S1). Genome size
152 prediction using k-mers distribution spectra predicted a genome of 308 Mb, concordant
153 with the assembly size (Figure S1). Such a genome size is significantly larger than the
154 remaining drosophilid species (Student's *t* one-sample test $P < 1.3 \times 10^{-4}$; Shapiro-Wilk
155 normality test $P = 0.55$). Phylogenetic analysis of genome size evolution indicates that the
156 *B. coeca* genome likely retained the size of the ancestral Steganinae, *i.e.* a stronger
157 reduction occurred in the Drosophilinae lineage containing *D. melanogaster* (Figure 2B;
158 Figure S2; Table S1).

159 To determine the number of protein-coding genes, we used four rounds of Maker³³
160 supported by the training of the gene finding and prediction tools SNAP³⁴ and Augustus³⁵.
161 The annotation, made on the repeat-masked genome, yielded 10,349 protein-coding
162 genes with an Annotation Edit Distance (AED) ≤ 0.5 for 96.4% of our gene models and a
163 Pfam domain found in 83.66% of the proteins (BUSCO score = 91%). Using the same
164 strategy, we annotated two steganine genomes, namely *Phortica variegata* and
165 *Leucophenga varia*. The annotation yielded 11,067 (BUSCO score = 91%) and 13,160
166 (BUSCO score = 90.8%) protein-coding genes, respectively. The annotation of the
167 ephydrid *Ephydra gracilis* genome yielded 9,154 protein-coding genes (BUSCO score =
168 68.9%) (Figure S2). *Ephydra* is particular among Ephydroidea in adapting to hypersaline
169 waters and associated algal flora.³⁶ Given the current low knowledge of ephydrid genetics,
170 whether their low gene content is due to their high specialization or an artifact of
171 incomplete annotation, is hard to know. Regardless, the bee louse fly has the lowest
172 number of protein-coding-genes compared to other drosophilids (Student's *t* one-sample

173 test $P < 1.5 \times 10^{-5}$; Shapiro-Wilk normality test $P = 0.48$) despite having a total genome
174 size that is among the largest genomes in the family. Whereas the near-completeness of
175 our *B. coeca* genome (~95%) might have reduced the number of annotated genes, low
176 complexity hard-to-assemble genomic regions are usually mostly heterochromatic and
177 poor in genes, e.g., centromeres, Y chromosomes, etc. A low gene content is also
178 characteristic of bee genomes, compared to ants and wasps, with a remarkable trend of
179 gene reduction within the family Apidae during the evolution of the genus *Apis* (Figure
180 2C; Figure S2; Table S1).

181

182 *Transposable elements (TEs) expanded in the bee louse fly with one element horizontally*
183 *transferred with the host*

184 The bee louse fly's large genome size and low gene content suggest an increase in
185 repetitive sequences. RepeatModeler and RepeatMasker analyses^{37,38} indicated that
186 nearly 41.34% of the *B. coeca* genome consists of such sequences, compared to 22.05%
187 and 10.98% in *D. melanogaster* and *A. mellifera*, respectively (Figure 2D). Remarkably,
188 half of the bee louse fly repetitive sequences consisted of long interspersed nuclear
189 elements (LINEs) retrotransposons (14.94%). While LINEs are usually among the most
190 abundant transposable elements after LTRs within the Drosophilidae,³⁹ their values did
191 not exceed what was found in *B. coeca* (we found the highest percentage in *Leucophenga*
192 *varia* with 5.54%). It is at present unclear what factors influence the diversity of
193 transposable elements (TEs) landscapes among eukaryote species⁴⁰. Nonetheless, this
194 difference means that whereas the bee louse fly has likely retained the ancestral large
195 genome size of the Drosophilidae, its TEs constitution has largely evolved.

196 Because host-parasite relationships have repeatedly been invoked as a factor that
197 may favor horizontal transfer of TEs,⁴¹ we searched for evidence of such transfers
198 between *B. coeca* and *A. mellifera*. We found one TE, a DNA transposon *Famar1-like*
199 element previously described in the earwig *Forficula auricularia*⁴² that belongs to the Tc1-
200 mariner superfamily. This element showed a high similarity between *B. coeca* and *A.*
201 *mellifera* but was absent in all other drosophilid species for which a genome is available
202 in GenBank, which is highly suggestive of an acquisition through horizontal transfer
203 (Figure S2). Indeed, phylogenetic analysis of multiple copies of this TE extracted from 37
204 widely divergent animal species (Figure 2E) supported a direct transfer event between *B.*
205 *coeca* and *A. mellifera*, although the directionality of the transfer cannot be inferred since

206 the elements from the two species form mutually-exclusive monophyletic clades.
207 Remarkably, all elements found in the genomes of four *A. mellifera* subspecies, including
208 *A. m. carnica*, *A. m. caucasia*, *A. m. mellifera* and *A. m. ligustica*, formed an exclusively
209 monophyletic clade. The transfer time between *B. coeca* and *A. mellifera* has likely
210 preceded the dispersion of this element among the subspecies or even their
211 differentiation 0.77 myr ago⁴³ if the element was ancestral in *A. mellifera*. On the other
212 hand, we did not find any trace of this element or any other related element in any other
213 *Apis* species, indicating that the maximal time of horizontal transfer likely does not
214 surpass 2.73 [0.70-8.9] myr ago, *i.e.* the time of divergence between *A. mellifera* and its
215 closest-relative *A. cerana* (Figure 2A). The tight ecological connection between the bee
216 louse fly and its host may have favored this transfer, as was suggested for blood- or sap-
217 sucking insects.^{44,45}

218

219 *Gene families with excess losses show striking cross-order parallelism*

220 Despite their deep divergence, we tested whether parallel changes could explain
221 the reduction of protein-coding genes in both the honey bee and the bee louse fly. We used
222 OrthoFinder⁴⁶ to cluster orthologous proteins from the 25 hymenopteran and 17 dipteran
223 species. We identified 19,010 orthogroups. Of these, 935 showed significant size evolution
224 among the 42 species when analyzed using CAFE5⁴⁷ and after applying an error model
225 that accounted for misassemblies and misannotations. To classify those orthogroups into
226 functional categories, we extracted groups that contained *D. melanogaster* orthologs for
227 which a molecular function, *i.e.* a gene group, was assigned in the Flybase database⁴⁸ (see
228 Methods). Of 1,078 gene groups, 136 significantly deviated from the birth-death model
229 estimated by CAFE5.

230 After correction for multiple testing, 17 gene groups had significant losses in the
231 bee louse fly with no group showing significant gain (Table 1). The reduction of most of
232 these groups showed a striking parallelism with bees (Anthophila) in particular and
233 hymenopterans in general (Table 1, Figure S3). The most significant groups were those
234 involved in the chemical detection of taste (gustatory receptors and divergent ionotropic
235 receptors) and odors (odorant receptors and odorant binding proteins). The remaining
236 groups included those involved in recognition and signaling with a potential role in
237 metabolism, immunity, and/or development such as C-type lectins, serine proteases, and
238 Dorsal,⁴⁶ as well as ion and sugar transportations. Other groups are involved in

239 detoxification, such as cytochrome P450, GST-C, and carboxylases.⁴⁷ Indeed, bees have
240 evolved a reduced repertoire of immunity and detoxification genes, likely due to the
241 evolution of social behavior and their life in an overprotective and clean shelter, *i.e.* the
242 nest.^{49,50} Cytochrome P450 genes are more expressed in foraging workers than in the
243 castes that remain in the nest (*i.e.* the queen and nurse workers).⁵¹ The reduction of
244 peptidases in both the honey bee and the bee louse fly could also be due to the low protein
245 content of some of their food, *i.e.* nectar and honey. We also noted an underrepresentation
246 of chitin-binding domain proteins and chitinases in the bee louse fly and the honey bee.
247 Cuticles could act as barriers against environmental toxins, which may not be highly
248 encountered in the nest. Remarkably, *B. coeca* is unique among cyclorrhaphan dipterans
249 as its pupa, similarly to the honey bee's,⁵² is contained in the unmodified cuticle of the
250 third instar larva, and no sclerotized puparium is formed.^{6,7} Whereas assembly and
251 annotation errors can bias general estimates of gene losses, they should not specifically
252 target the gene families that are ecologically relevant to both the host and the inquiline.

253

254 *Honey and wax feeding drove the loss of almost all bitter-tasting gustatory receptors*

255 The two most significantly evolving gene families in the bee louse fly, *i.e.* gustatory
256 receptors (GRs) and divergent ionotropic receptors (IR-DIVs), allow the detection of
257 soluble cues (Table 1). There are 60 GRs in *D. melanogaster*, of which 9 and 49 receptors
258 respond primarily to sweet and bitter tastes, respectively, and 2 receptors respond to
259 carbon dioxide (CO₂).⁵³ The three categories clustered into 35 orthogroups (Figure 3A),
260 whose phylogenetic analysis indicates that the ancestral drosophilid repertoire consisted
261 of 6 sweet, 26 bitter, and 2 CO₂ GRs assuming functional conservation of gustatory
262 categories (Figure 3A). We identified 11 GRs in the bee louse fly with no duplications
263 using InsectOR⁵⁴ and manual curation. These GRs could be classified according to their *D.*
264 *melanogaster* orthologs into 3 sweet, 6 bitter, and 2 CO₂. That means that the *D.*
265 *melanogaster* lineage disproportionally evolved more bitter receptors from the ancestral
266 repertoire, whereas *B. coeca* disproportionally lost bitter receptors (Figure 3A). InsectOR
267 inferred the number of GRs in the steganine species *L. varia* and *P. variegata* to be 21 and
268 26, respectively, further confirming that *B. coeca* has lost a significant portion of the
269 ancestral GR repertoire (Figure S4). Honey bees have only 11 GRs, of which 7 are
270 orthologous to sweet *Drosophila* GRs.⁵⁵ This is likely due to the bees' strong diet reliance

271 on sweet floral nectars and honey.⁵⁶ The loss of *B. coeca* bitter GRs and its retention of 2
272 ancestral sweet receptors is a strong convergence with its host.

273 Ionotropic receptors are another major class of chemoreceptors. They are divided
274 into antennal IRs, which are conserved across insects and are most likely involved in
275 olfaction, and divergent IRs (IR-DIVs), which evolve rapidly and are mostly involved in
276 the taste perception of carboxylic and amino acids. Only divergent IRs showed a
277 significant loss in *B. coeca* (Table 1). However, our knowledge about the function of the
278 42 *D. melanogaster* IR-DIVs is still limited.⁵⁷ We inferred the ancestral IR-DIV drosophilid
279 repertoire to contain 29 receptors, of which only 9 were retained in *B. coeca*. Remarkably,
280 whereas we found almost no direct orthologs between Diptera and Hymenoptera for IR-
281 DIVs (Figure S3), bees are known to have few IRs in general⁵⁸ pointing to another possible
282 taste convergence between the bee louse fly and its host.

283

284 *One-fifth of ancestral odorant receptors was lost, including one receptor that is involved in*
285 *anti-ovarian response in Drosophila melanogaster*

286 Odorant receptors (ORs) are essential to detect volatile chemical cues from the
287 environment. This family has expanded in the honey bee to reach 170.⁵⁹ However, only 9
288 of the honey bee genes have orthologs with *D. melanogaster*, and phylogenetic analysis
289 indicates that this common OR repertoire has been gradually reduced during the
290 evolution of *Apis* (Table 1, Figure S3). The 60 ORs of *D. melanogaster* clustered within 16
291 orthogroups (Figure 3B). We inferred the ancestral drosophilid OR repertoire to contain
292 44 ORs, with at least one representative for each orthogroup (Figure 3B). We identified in
293 *B. coeca*, following InsectOR⁵⁴ and manual curation, 35 ORs in addition to *Orco*, i.e. one-
294 fifth of the ancestral repertoire was lost. The number of ORs was 50 and 51 in the two
295 closely related steganine species *L. varia* and *P. varia*, respectively (Figure S4). *Braula* ORs
296 were direct orthologs to 18 genes in *D. melanogaster* (Figure 3B). Judging from the
297 response of these orthologs to different volatiles in *D. melanogaster* as curated in the
298 DoOR database⁶⁰ and assuming potential conservation of function, the retained bee louse
299 fly ORs may respond to compounds produced by honey bee workers in a defense context
300 (e.g., 1-hexanol, farnesol, 2-heptanone),⁶¹ and/or of floral, pollen and nectar aromas, such
301 as acetophenone and benzaldehyde, a major volatile of honey.^{62,63} Two cases of
302 tetraplications were observed. One case involved three recent duplications of genes
303 orthologous to DmOr67b, a gene that is highly responsive in *D. melanogaster* to both

304 acetophenone and 1-hexanol. The second case involved three successive duplications of
305 a gene orthologous to DmOr74a, which responds in *D. melanogaster* larvae to 1-nonanol
306 and 1-heptanol, the latter being a major brood volatile,⁶⁴ and 1-hexanol, a component of
307 the alarm pheromone.⁶⁵ Of these three duplications, two were unique to *B. coeca*
308 compared to its closely-related steganine species (Figure S4). Low concentrations of
309 isopentyl acetate, the main component of the alarm pheromone, released by unstressed
310 workers at the nest entrances attract the parasitic nest beetle *Aethina tumida*,⁶⁶
311 suggesting that the detection of the host odors could be a common strategy among
312 phylogenetically distant inquilines and parasites of social insects.

313 Whereas major molecular convergences could exist between the inquiline and its
314 social host, divergent strategies to adapt to the eusocial lifestyle requirements are still
315 needed. In honey bees, colony cohesion is driven by the volatile queen's mandibular
316 pheromone (QMP), which "sterilizes" the bee workers.⁶⁷ This pheromone elicits an anti-
317 ovarian response in other insects, including *D. melanogaster*.²⁸ An RNA interference
318 (RNAi)-screen identified DmOr49b, DmOr56a, and DmOr98a to be potentially involved in
319 the detection of the QMP compounds and the suppression of fecundity.^{28,68} A *sine qua non*
320 condition for a drosophilid to reproduce in a bee nest would, therefore, be to lose those
321 receptors or to modify their response or effect. We found that the bee louse fly does not
322 have an ortholog for DmOr98a, a receptor specific to the genus *Drosophila* (Figure S4).
323 The bee louse fly has a pseudogene, orthologous to DmOr49b, that InsectOR identified.
324 Orthologs of this *D. melanogaster* receptor are present and complete in all dipteran
325 species, including *L. varia* and *P. variegata* (Figure S4). The bee louse fly had a receptor
326 that we called BcOr22, which was orthologous to DmOr56a (Figure 4B). This last receptor
327 is narrowly tuned in many *Drosophila* species to a single component, the mold volatile
328 geosmin, whose perception also inhibits oviposition in *D. melanogaster*,⁶⁹ pointing to a
329 possible conserved role in reproduction. Therefore, further functional analyses of the
330 response of candidate ORs to various QMP compounds are required in both *D.*
331 *melanogaster* and *B. coeca* to understand how modifications of these genes in *B. coeca*
332 might have facilitated the evolution of the bee louse fly inquilinism.

333

334 *Blindness and life in a dark nest were accompanied by the loss of multiple rhodopsins*

335 The species Latin name of the bee louse fly refers to the assumption that it was
336 blind due to the reduction of the eye size and the loss of the ocelli. In agreement with

337 reduced vision in the bee louse fly, we found only two out of the seven rhodopsin genes,
338 which are responsible for colored vision and positive phototaxis in *D. melanogaster* and
339 which were all present in the ancestral drosophilid repertoire. *D. melanogaster* orthologs
340 of the *Rh1* and *Rh6* genes are expressed in the ommatidia and are sensitive to light.⁷⁰ The
341 role of these opsins in light detection, despite the absence of ommatidia in the bee louse
342 fly is unclear. Remarkably, *Rh1* and *Rh6* are structurally required in mechanosensory
343 bristles to control larval locomotion.⁷¹ They also detect temperature.⁷² Therefore, the
344 retention of these rhodopsins in the bee louse fly could mainly be due to their
345 unconventional functions. On the other hand, the rhodopsin *Rh2*, which is exclusively
346 expressed in the ocelli and used for horizon detection in *D. melanogaster*⁷³, is among
347 those lost in the bee louse fly, in agreement with the loss of the ocelli. Regression of the
348 visual system and its underlying opsin genes is common in animals inhabiting dark
349 environments, such as fossorial mammals⁷⁴ and cavefishes,⁷⁵ representing a major
350 example of deep convergences.

351

352 *Apterism was not accompanied by the loss of major wing development genes*

353 Small size, loss of wings, and the evolution of strongly clinging legs are all
354 morphological changes that could prevent the honey bees from getting rid of the bee
355 lice.⁷⁶ All these potential adaptations are convergent with ectoparasitic true lice, and for
356 some, such as apterism, represent major recurrent changes that have responded to
357 distinct pressures throughout the history of insects.⁷⁷ We found intact most of the main
358 wing development genes whose mutations severely reduce the wing in *D. melanogaster*,
359 such as *wingless*, *apterous*, or *vestigial*. This means that the major morphological changes
360 more likely resulted from regulatory changes of these core genes or modifications of other
361 genes. Future developmental studies, specifically comparing the expression of wing and
362 leg morphogenic genes between the bee louse fly and *D. melanogaster*, will definitively
363 help shed light on the transcriptomic shifts underlying the major morphological changes
364 of the bee louse fly.

365

366 **Conclusion**

367 That the enigmatic bee louse fly is indeed a drosophilid, a lineage within the most
368 investigated insect family with more than 150 fully sequenced genomes, is undoubtedly
369 one of the most exciting discoveries in dipteran phylogeny. How could a fly with an

370 ancestral drosophilid genome become ecologically adapted to bees and morphologically
371 similar to lice? Our results show that a mosaic of deep convergences at the genomic level
372 underlies the relatively recent and dramatic changes of the bee louse fly to nest
373 inquilinism. This mosaicism involved deep convergences with the host, mostly in genes
374 likely involved in immunity, detoxification, and chemical perception, as well as
375 convergences with general features of fossorial animals in the visual systems. Future
376 developmental studies may elucidate whether general morphologies, such as apterism
377 and leg modifications, could also be shared between *Braula* and other ectoparasites. Due
378 to its genetic relatedness to *Drosophila* and ecological association to *Apis*, two major
379 laboratory models, the new genomic resources presented here can help establish the bee
380 louse fly as a promising model to address questions related to deep convergences that are
381 difficult to approach in multiple highly specializing animals.

382

383 **Acknowledgments**

384 We are very grateful to Marcus Stensmyr for insightful comments on an early draft of the
385 manuscript, the *Association Conservatoire de l'Abeille Noire Bretonne* (A.C.A.N.B.) for help
386 collecting *B. coeca* flies, Etienne Minaud for photographic images of *B. coeca* and Héloïse
387 Muller for help with the genome annotation pipeline, Christian Cheminade and Michael
388 Lang for help translating early literature on *Braula*. *Braula* genome sequencing was
389 funded by a grant from Université Paris-Saclay (ADAPAR) to HB.

390

391 **Author contributions**

392 Conceptualization: H.B. and A.Y. ; Investigation: H.B., H.L., N.D., D.O., C.P., J.F., C.G., and A.Y.;
393 Resources: H.L. and L.G.; Writing – Original draft: H.B., H.L., D.O., J.F., C.G., and A.Y.; Writing
394 – Reviewing & Editing: H.B., J.C., C.G., F.M.P., F.R., J.C.S., and A.Y.; Visualization: H.B., J.F.,
395 C.G., and A.Y.; Supervision: H.B.; Funding Acquisition: H.B.

396

397 **Declaration of interests**

398 The authors declare no competing interests.

399

400 **Declaration of generative AI and AI-assisted technologies in the writing process**

401 During the preparation of this work the authors used Grammarly (Grammarly Inc.) in
402 order to improve language and readability. After using this tool/service, the authors

403 reviewed and edited the content as needed and take full responsibility for the content of
404 the publication.

405

406 **Figures titles and legends**

407

408 **Figure 1. The bee louse fly (*Braula coeca*) is an inquiline of the Western honey bee**
409 **(*Apis mellifera*) and has likely evolved from a sap-breeding drosophilid associated**
410 **with scale insects. See also Table S1.**

411 **(A)** Tens of *B. coeca* adults preferentially attached to the honey bee queen (© Etienne
412 Minaud). Scale bar = 5 mm.

413 **(B)** Dorsal view of an adult showing the loss of the wings, halteres, and scutum, mesonotum
414 reduction and the legs' robustness. Scale bar = 0.5 mm.

415 **(C)** Frontal view of an adult showing the reduction of the eyes and the loss of the ocelli.
416 Scale bar = 0.5 mm.

417 **(D)** Maximum likelihood phylogeny inferred from 3,100 conserved single-copy proteins
418 (2,557,349 amino acids) showing the position of *B. coeca* (orange) in the subfamily
419 Steganinae (light green) of the Drosophilidae (red). Outgroup species belong to the
420 superfamily Ephydroidea (light blue). All internal nodes had an ultra-fast bootstrap value
421 of 100% except * = 73%. Pie charts at internal nodes indicate the likelihood of ancestral
422 breeding niches inferred from the predominant niches of terminal taxa.

423

424 **Figure 2. Evolution of the bee louse fly inquilinism, its genome size, gene content,**
425 **and transposable elements in the bee louse fly with evidence for horizontal transfer**
426 **between the inquiline and its host. See also Table S1 and Figure S2.**

427 **(A)** Fossil-calibrated maximum-likelihood phylogeny inferred from 79 conserved single-
428 copy proteins (63,192 amino acids) demonstrating major stages in the evolution of the
429 inquiline and its social host. All internal nodes had an ultra-fast bootstrap value of 100
430 (except when given), with a blue interval indicating a 95% confidence level of divergence
431 time estimate inferred by MCMCTree. The red bar indicates the likely interval of the origin
432 of the bee louse fly-*Apis* association. Labels 1-6 refer to the major stages mentioned in the
433 text.

434 **(B)** Genome-size evolution. Red asterisk indicates the estimate for *B. coeca*.

435 **(C)** Gene content evolution. Red asterisk indicates the estimate for *B. coeca*.

436 **(D)** Proportions of transposable elements in the genomes of 42 dipteran and
437 hymenopteran species. DNAs = DNA transposons, LCs = low complexity elements, LINEs
438 = long interspersed nuclear elements, LTRs = long terminal repeats, SINEs = short
439 interspersed nuclear elements, sRNAs = small RNAs, SRs = single repeats, and Unclass. =
440 unclassified.

441 **(E)** Maximum-likelihood phylogeny of *Famar1*-like copies from 38 animal species. Filled
442 circles indicate ultrafast bootstrap values higher than 90%.

443

444 **Figure 3. Evolution of chemosensory receptors gene families in *Braula coeca* and**
445 ***Drosophila melanogaster*. See also Figure S4.**

446 **(A)** Maximum-likelihood phylogeny of gustatory receptors (GRs) with main taste
447 categories color code given in a frame.

448 **(B)** Maximum-likelihood phylogeny of odorant receptors (ORs) with main ligands for
449 each *D. melanogaster* receptor given in dark red. L = larva and A = adult expression.

450 For A and B, ultra-fast bootstrap values are given above nodes. Branches are colored
451 according to orthogroups defined by OrthoFinder for 42 dipteran and hymenopteran
452 species. Numbers in broken brackets before each orthogroup reflect the presumed
453 ancestral gene content inferred by phytools.

454

455 **STAR Methods**

456 RESOURCE AVAILABILITY

457 **Lead contact**

458 Further information and requests for resources and reagents should be directed to and
459 will be fulfilled by the lead contact, Héloïse Bastide ([heloise.bastide@universite-paris-](mailto:heloise.bastide@universite-paris-saclay.fr)
460 [saclay.fr](mailto:heloise.bastide@universite-paris-saclay.fr)).

461 **Materials availability**

462 This study did not generate new unique reagents.

463 **Data and code availability**

464 • Raw sequence data are deposited on NCBI Sequence Read Archive (SRA).
465 Bioproject accession number is listed in the key resources table. Genome
466 assemblies and all data associated to this study including translation of early
467 taxonomic literature are deposited in Figshare. DOI is listed in the key resource
468 table.

- 469 • All original code and commands for all programs have been deposited at Github
470 depository. DOIs are listed in the key resource table.
- 471 • Any additional information required to reanalyze the data reported in this paper
472 is available from the lead contact upon request.

473

474 EXPERIMENTAL MODEL AND SUBJECT DETAILS

475 ***Sample collection and genomic library preparation***

476 Samples of *Braula coeca* were collected from honey bee colonies on the Island of
477 Ouessant in France and kindly provided to us by the *Association Conservatoire de l'Abeille*
478 *Noire Bretonne* (A.C.A.N.B.). Genomic DNA was extracted from 15 unsexed individuals
479 conserved in alcohol using the Nucleobond AXG20 kit and buffer set IV from Macherey-
480 Nagel (ref. 740544 and 740604, <https://www.mn-net.com>, Düren, Germany).

481

482 METHOD DETAILS

483 ***Genome sequencing and assembly***

484 We used a hybrid approach to assemble a draft genome of *B. coeca* using both long-
485 read Oxford Nanopore Technology (ONT) and short-read Illumina sequencing.⁷⁸ Before
486 nanopore sequencing, a size selection was conducted on the DNA using the SRE XS kit
487 from Circulomics (<https://www.circulomics.com/>, Baltimore, Maryland, USA). The
488 Ligation Sequencing kit SQK-LSK110 from ONT (<https://nanoporetech.com/>)⁷⁹ was then
489 used to prepare the samples for nanopore sequencing following the manufacturer's
490 protocol. The library was loaded and sequenced on an R9.4.1 flow cell (ref. FLO-Min106)
491 for sequencing. Raw data were basecalled using Guppy v5.0.11 and the "sup" algorithm.
492 The ONT raw data size was 4.4 Gb in 1,399,323 reads (mean read length 3,146 kb, longest
493 read of 123.3 Mb), with an N50 of 4,677 kb. Phred scores ranged from 8 to 18, with a
494 median of 13, as assessed by PycoQC.⁸⁰ Illumina paired-end sequencing was performed
495 by Novogene Company Limited (<https://en.novogene.com>, Cambridge, UK) on the same
496 DNA sample. The Illumina sequencing produced 119,719,537 paired 150 bp reads. Phred
497 scores averaged 36 per read as analyzed by FastQC
498 (<http://www.bioinformatics.babraham.ac.uk/projects/fastqc/>). We used MaSuRCA
499 v4.0.3⁸¹ to produce the hybrid assembly of our genome using the Cabog assembler. We
500 obtained a final assembly size of 309,35Mb in 2477 contigs, with a N50 of 347,227 bp. The
501 completeness of the assembly was estimated to 95.8% with BUSCO v5.0.0 on the

502 *diptera_odb10* dataset (C:95.8%[S:94.5%,D:1.3%],F:0.7%,M:3.5%,n:3285), and to 93.6%
503 using Merqury.

504 ***Estimation of genome size and endosymbionts detection***

505 K-mers frequencies within short-read data were obtained with KMC 3.⁸² Genome
506 size and ploidy were inferred using GenomeScope v2.0 with k-mer size = 21 and
507 Smudgeplot.⁸³ Contig taxonomy was performed using Blobtools⁸⁴ with Diamond as search
508 engine⁸⁵ against the UniProt database using a local copy of the NCBI TaxID file for the
509 taxonomic assignation of the best hit. Minimap2⁸⁶ was used for read mapping (Figure S1).

510 ***Genome annotation***

511 The *B. coeca* genome was annotated using Maker v2.31.10,³³ following Muller et
512 al.'s⁸⁷ protocol, wherein multiple rounds of Maker supported by the training of the SNAP
513 v.2006-07-28³⁴ and Augustus v.3.3.3³⁵ gene finding and prediction tools, were conducted.
514 RepeatModeler v2.0.1 was first used to identify the repeat-enriched regions that were
515 masked by RepeatMasker v4.0.9 as implemented in Maker. Proteomes of five *Drosophila*
516 species, namely *D. innubila*, *D. albomicans*, *D. bipectinata*, *D. melanogaster*, and *D. virilis*
517 were obtained from NCBI and used to guide the annotation. Protein-Protein BLAST
518 2.9.0+⁸⁸ (-evaluate 1e-6 -max_hsps 1 -max_target_seqs 1) was then used to assess putative
519 protein functions in *B. coeca* by comparing the protein sequences given by Maker to the
520 protein sequences from the annotated genome of *D. melanogaster*. The completeness of
521 genome annotation was assessed using BUSCO at each round and the round with the
522 highest score was retained.

523 ***Phylogenomic analysis of the Ephydroidea***

524 Besides our *B. coeca* assembly, we obtained from NCBI repository genome
525 assemblies for 12 species, transcriptome shotgun assemblies (TSA) for four species, and
526 sequence read runs (SRR) for three species (Table S1). Paired-end DNA raw data of two
527 species, namely *Rhinoleucophenga* cf. *bivisualis* and *Cacoxenus indagator* were assembled
528 using MaSuRCA with default parameters. The transcriptome of *Acletoxenus* sp. was
529 assembled using Trinity software package⁸⁹ on the Galaxy Europe website⁹⁰ following
530 standard protocol⁹¹. BUSCO v.5.0 was used to assess the completeness of those assemblies
531 and to extract single-copy BUSCO genes for all species. Protein sequences of 3,100 single
532 and complete BUSCO genes were aligned using MAFFT⁹² and concatenated into a single
533 supermatrix (2,557,349 amino acids). A maximum-likelihood (ML) phylogeny was then
534 inferred for the supermatrix using IqTREE 2⁹³ with 1,000 ultrafast bootstrap iterations⁹⁴

535 and using the JTT+R substitution model inferred by ModelFinder⁹⁵ implemented by
536 IqTree.

537 ***Reconstruction of the ancestral ecological niches***

538 For each of the 20 ephydroid species we obtained a predominant ecological niche
539 from the taxonomic literature.^{20,23,24,96} Eight predominant niches were coded as discrete
540 traits, and the Multistate program of the BayesTraits v.4 package⁹⁷ was used under the
541 Reverse Jump MCMC model with 1,010,000 chain iterations and a burnin sample of
542 10,000.

543 ***Phylogenomic analysis of Diptera and Hymenoptera***

544 The second phylogenomic analysis involved, besides *B. coeca*, 25 hymenopteran
545 and 16 dipteran species for which an assembly can be downloaded from the NCBI Genome
546 repository (Table S1). Protein sequences for all species but three, namely *Leucophenga*
547 *varia*, *Phortica variegata*, and *Ephydra gracilis*, were obtained from NCBI. For these three
548 species, we used the same four-round annotation procedure that we used for *B. coeca* to
549 identify protein-coding genes and translate their sequences. We used BUSCO to assess the
550 completeness of all annotated and downloaded genomes and their corresponding
551 assemblies. OrthoFinder⁴⁶ was used to generate protein sequences of protein-coding-
552 genes of the 42 species and to cluster these sequences into orthogroups. Only the longest
553 isoform (*i.e.* the primary transcript) was used for genes with multiple isoforms. 79
554 orthogroups contained a single copy ortholog from each species, and their protein
555 sequences were aligned using MAFFT and concatenated into a single supermatrix (63,192
556 amino acids). A maximum-likelihood (ML) phylogeny was then inferred for the
557 supermatrix using IqTREE 2⁹³ with 1,000 ultrafast bootstrap iterations⁹⁴ and the JTT+R
558 substitution model inferred by ModelFinder⁹⁵ implemented by IqTree.

559 MCMCTree⁹⁸ was used to date the inferred ML trees based on recently published
560 fossil-calibrated phylogenies. First, two time points were obtained for the 42-species
561 phylogeny. These included the divergence between ants and bees between 90-120 myr
562 ago⁹⁹ and between *Scaptodrosophila* and *Drosophila* between 50-56 myr ago,¹⁰⁰ with a
563 maximum root age for the ancestor of Hymenoptera and Diptera at 344 myr ago.⁹⁹

564 ***Genome size and gene content evolution***

565 Genome size and gene content (number of OrthoFinder generated protein-coding-
566 genes after retaining the longest isoform for genes with multiple transcripts) inferred for
567 each of the 42 dipteran and hymenopteran genomes were mapped on the phylogenetic

568 tree, and values at the ancestral nodes were inferred and visualized using the fastAnc
569 command in the R package Phytools v0.2.2.¹⁰¹

570 ***Transposons annotation and detection of Horizontal Transposon Transfer (HTT)***

571 Transposons were identified in the 42 dipteran and hymenopteran genomes
572 following a two-step protocol. First, we used RepeatModeler v2.0.1³⁷ with default
573 parameters to generate a *de novo* library of repetitive regions. RepeatMasker v 4.0.9³⁷ was
574 then run with the newly generated library and the options -a (create a .align output file)
575 and -s (slow search; more sensitive) to create a summary of the families of transposable
576 elements found in each genome along with the percentage of the genome they represent.
577 To detect possible HTT between *Braula coeca* and *Apis mellifera*, we used the *B. coeca*
578 whole genome as query to perform a blastn similarity search against the whole *A.*
579 *mellifera* genome (all default options, including “-task megablast”). All *B. coeca* genome
580 regions longer than 299 bp and aligning to *A. mellifera* with an e-value lower than 0.0001
581 were extracted and clustered at 80% nucleotide identity threshold with vsearch.¹⁰² The
582 consensus sequence of each of the 50 resulting clusters were used as queries to perform
583 blastx searches on the non-redundant protein database of NCBI using Diamond.⁸⁵ A total
584 of eight consensus sequences had best hits to the *Famar1* element previously described
585 in the earwig *Forficula auricularia*, known to be also present in *A. mellifera* as a result of
586 horizontal transfer.^{42,103} To verify that the *Famar1*-like element from *B. coeca* has indeed
587 been involved in HTT, we compared the *Famar1*-like synonymous distance (dS) to a
588 distribution of dS expected under vertical transmission since the last common ancestor
589 of *B. coeca* and *A. mellifera* following the approach developed in Zhang *et al.*¹⁰⁴ This
590 approach assumes that in case of HTT, TE dS should be much lower than dS expected
591 under vertical transmission. Briefly, we calculated the dS over the transposase open
592 reading frame between one copy of the *Famar1*-like element extracted from *C. coeca* and
593 another copy of this element from the *A. mellifera* genome. We then compared this
594 distance to the distribution of dS calculated over 2,179 alignments between single copy
595 BUSCO genes that produce best reciprocal hits in blastp similarity searches.¹⁰⁴ We found
596 that the *Famar1*-like dS (=0.12) fall below the 0.5% quantile (=1.76) of the distribution of
597 dS calculated for orthologous genes (Figure S2), confirming that the element has been
598 acquired through HTT in *B. coeca* and *A. mellifera*. To assess whether the tight ecological
599 interactions existing between *B. coeca* and *A. mellifera* might have favored direct transfer
600 of this element between the two species, we assessed how closely related are *B. coeca*

601 *Famar1*-like copies to those from *A. mellifera*. We first screened for the presence of this
602 element in other animal genomes. We used the *Famar1* sequence⁴² as query to perform
603 online blastn similarity searches (all default options, including “-task megablast”) on a
604 total of 8,180 animal genomes belonging to 11 insect orders as well as to Annelida,
605 Chelicerata, Chiroptera, Cnidaria, Myriapoda, Nematoda, Platyhelminthes and Teleostei.
606 We found full length copies showing >79% of nucleotide identity to this element in a total
607 of 37 species. We aligned up to ten copies from each genome the most similar to *Famar1*
608 using Muscle.¹⁰⁵ We then reconstructed a maximum-likelihood phylogeny of these copies
609 using IqTree after nucleotide model detection using ModelFinder. Node support was
610 quantified using ultrafast bootstrap as implemented in IqTree.

611 ***Gene family evolution***

612 We used CAFE v. 5⁴⁷ to model and infer gene family evolution. We conducted
613 CAFE5 using an error model on the 19,011 orthogroups generated by OrthoFinder and
614 using the time-calibrated phylogenetic tree of the 42 dipteran and hymenopteran species.
615 The analysis showed that *B. coeca* has gained 439 while losing 1,517 protein-coding genes
616 in agreement with the low gene content of this species. To gain further functional insights
617 on the ecological or biological relevance of the evolving genes, we grouped OrthoFinder
618 orthogroups into functional gene groups using the customized perl script OG2GG.pl
619 (<https://github.com/AmirYassinLab/OG2GG>) leveraging the proximity of *B. coeca* to *D.*
620 *melanogaster*. The script assigns each *D. melanogaster* ortholog to its largest functional
621 gene groups in Flybase⁴⁸ (“gene_group_data_fb_2023_02.tsv”) and then assigns each
622 orthogroup to the largest gene group of its constituent genes. *D. melanogaster* has 13,545
623 protein-coding genes that were clustered into 10,497 orthogroups. However, 8,202 *D.*
624 *melanogaster* genes are assigned to at least one of 10,670 functional gene groups in the
625 FlyBase database, of which some concern RNA genes that, by definition, are not analyzed
626 by OrthoFinder. Because of the hierarchical nature of the functional gene groups
627 annotation in FlyBase as well as to the pleiotropy of certain genes, each *D. melanogaster*
628 gene was assigned to its largest group, *i.e.* the group with biggest number of genes.
629 Consequently, 5,733 protein-coding genes were assigned to an orthogroup and a gene
630 group. Because some orthogroups can have multiple genes with some assigned to
631 different gene groups, each orthogroup was assigned to the largest gene group of its
632 constituent genes. Orthogroups were then clustered according to their assigned
633 functional groups, e.g., the odorant receptors family contained 16 orthogroups (and 60 *D.*

634 *melanogaster* genes). Because some of the genes found in the orthogroups based on their
635 sequence similarity have no functional annotation in Flybase, the total number of *D.*
636 *melanogaster* protein-coding genes to be grouped into gene groups was 7,820 genes (and
637 6,317 protein-coding genes for *B. coeca*).

638 CAFE5 was then run on the gene groups' gene counts using four different birth rate
639 models in an increasing order ($\lambda = 1, 2, 3$ and 4) and the error model to correct for
640 possible assembly and annotation errors. For each model we run four iterations. The
641 likelihood of only the two simplest models, *i.e.* one- and two- λ models, converged
642 across the four iterations. Likelihood ratio test using the `lr.test` function of the `extRemes`
643 R package¹⁰⁶ showed that the two- λ better fit our data. This model imposed a
644 different rate for only *B. coeca* compared to the rest of the tree and it was chosen for four-
645 iterations of subsequent analyses using the estimated error rate. Multiple testing
646 corrections were conducted using the False Discovery Rate (FDR) analysis of the
647 `FDRestimation`¹⁰⁸ package implemented in R.

648 ***Chemosensory superfamilies evolution***

649 To curate *B. coeca* gustatory receptors (GR) and odorant receptors (OR) genes, we
650 queried *D. melanogaster* GRs and ORs protein sequences on *B. coeca*, *L. varia* and *P.*
651 *variegata* assemblies using Exonerate ver. 2.2¹⁰⁷ with option `-maxintron 2000` and `-p`
652 `pam250`. The output, along with the assembly, were fed to InsectOR⁵⁴ with option `7tm_7`
653 and `7tm_6` activated for GR and OR analyses, respectively. From the output files, we
654 extracted 300-500 amino acids-long complete sequences with `7tm_7` or `7tm_6` motif
655 detected and with start codon present and no internal stop codon, *i.e.* pseudogenes
656 excluded. Protein sequences were aligned using MAFFT and a maximum-likelihood
657 phylogenetic tree for each family using IqTREE 2 with the same options as the
658 phylogenomic analysis. The literature was reviewed to classify GRs into bitter, sweet, and
659 CO₂ categories¹⁰⁹ and identify volatile ligands eliciting the strongest response in odorant
660 neurons in *D. melanogaster*.⁶⁰ Because CAFE5 inferred ancestral counts for orthogroups
661 with significant deviation only, we estimated and visualized ancestral counts for each
662 orthogroups of these two families using `FastAnc` command in the R package `Phytools`.

663

664 QUANTIFICATION AND STATISTICAL ANALYSIS

665 ***Genome size and protein-coding gene content analyses***

666 We compared the estimates of genome size and protein-coding gene content of *B. coeca*
667 to the distributions of these values for the 10 drosophilid genomes (data given in Table
668 S1) using one-sample Student's *t* test and after testing for normality using Shapiro-Wilk
669 test as implemented in R.

670 **Likelihood Ratio Test (LTR) comparison of CAFE5 models**

671 We compared the likelihood of the two simplest CAFE5 models, *i.e.* one- and two-lambda
672 models which were the only ones to converge across the four iterations, using the `lr.test`
673 function of the `extRemes` R package.¹⁰⁶ For each model, the likelihood estimates were
674 averaged across the four iterations.

675 **False Discovery Rate (FDR) estimation of the p-values of the best CAFE5 model**

676 The two-lambda model had the best likelihood and was therefore subsequently run for
677 four iterations. *p*-values inferred for each gene group in the branch leading to *B. coeca* in
678 the iteration with the best likelihood were extracted, and multiple testing corrections
679 were conducted using the False Discovery Rate (FDR) analysis of the `FDReStimation`¹⁰⁸
680 package implemented in R.

681

682 **List of supplementary materials**

683

684 **Table S1.** List of all genome assemblies and annotations downloaded or generated in this
685 study with data on genome size, gene content and BUSCO scores.

686

687 **References**

- 688 1. Cini, A., Sumner, S., and Cervo, R. (2019). Inquiline social parasites as tools to unlock
689 the secrets of insect sociality. *Philosophical Transactions of the Royal Society B: Biological*
690 *Sciences* 374, 20180193. 10.1098/rstb.2018.0193.
- 691 2. Rabeling, C., Schultz, T.R., Pierce, N.E., and Bacci, M. (2014). A Social Parasite
692 Evolved Reproductive Isolation from Its Fungus-Growing Ant Host in Sympatry. *Current*
693 *Biology* 24, 2047–2052. 10.1016/j.cub.2014.07.048.
- 694 3. Borowiec, M.L., Cover, S.P., and Rabeling, C. (2021). The evolution of social
695 parasitism in *Formica* ants revealed by a global phylogeny. *Proceedings of the National*
696 *Academy of Sciences* 118, e2026029118. 10.1073/pnas.2026029118.
- 697 4. Dejean, A., Orivel, J., Azémar, F., Hérault, B., and Corbara, B. (2016). A cuckoo-like
698 parasitic moth leads African weaver ant colonies to their ruin. *Sci Rep* 6, 23778.
699 10.1038/srep23778.
- 700 5. Maruyama, M., and Parker, J. (2017). Deep-Time Convergence in Rove Beetle
701 Symbionts of Army Ants. *Current Biology* 27, 920–926. 10.1016/j.cub.2017.02.030.
- 702 6. Skaife, S.H. (1922). On *Braula Coeca*, Nitzsch, a Dipterous parasite of the honey bee.
703 *Transactions of the Royal Society of South Africa* 10, 41–48. 10.1080/00359192209519263.
- 704 7. Imms, A.D. (1942). On *Braula coeca* Nitsch and its affinities. *Parasitology* 34, 88–

- 705 100. 10.1017/S0031182000016012.
- 706 8. Bayless, K.M., Trautwein, M.D., Meusemann, K., Shin, S., Petersen, M., Donath, A.,
707 Podsiadlowski, L., Mayer, C., Niehuis, O., Peters, R.S., et al. (2021). Beyond *Drosophila*:
708 resolving the rapid radiation of schizophoran flies with phylotranscriptomics. *BMC Biol* 19,
709 23. 10.1186/s12915-020-00944-8.
- 710 9. Winkler, I.S., Kirk-Spriggs, A.H., Bayless, K.M., Soghigian, J., Meier, R., Pape, T.,
711 Yeates, D.K., Carvalho, A.B., Copeland, R.S., and Wiegmann, B.M. (2022). Phylogenetic
712 resolution of the fly superfamily Ephydroidea—Molecular systematics of the enigmatic and
713 diverse relatives of Drosophilidae. *PLOS ONE* 17, e0274292. 10.1371/journal.pone.0274292.
- 714 10. Avalos, J., Rosero, H., Maldonado, G., and Reynaldi, F.J. (2019). Honey bee louse
715 (*Braula schmitzi*) as a honey bee virus vector? *Journal of Apicultural Research* 58, 427–429.
716 10.1080/00218839.2019.1565726.
- 717 11. de Réaumur, R.-A.F. (1740). *Mémoires pour servir à l’histoire des insectes...* Vol. 5
718 (de l’Imprimerie royale).
- 719 12. Nitzsch, C. (1818). Die Familien und Gattungen der Thierinsekten (insecta epizoica);
720 als Prodromus einer Naturgeschichte derselben. In.
- 721 13. Simão, F.A., Waterhouse, R.M., Ioannidis, P., Kriventseva, E.V., and Zdobnov, E.M.
722 (2015). BUSCO: assessing genome assembly and annotation completeness with single-copy
723 orthologs. *Bioinformatics* 31, 3210–3212. 10.1093/bioinformatics/btv351.
- 724 14. Lewin, H.A., Robinson, G.E., Kress, W.J., Baker, W.J., Coddington, J., Crandall,
725 K.A., Durbin, R., Edwards, S.V., Forest, F., Gilbert, M.T.P., et al. (2018). Earth BioGenome
726 Project: Sequencing life for the future of life. *Proceedings of the National Academy of*
727 *Sciences* 115, 4325–4333. 10.1073/pnas.1720115115.
- 728 15. Rhie, A., Walenz, B.P., Koren, S., and Phillippy, A.M. (2020). Merqury: reference-
729 free quality, completeness, and phasing assessment for genome assemblies. *Genome Biology*
730 21, 245. 10.1186/s13059-020-02134-9.
- 731 16. Koren, S., Phillippy, A.M., Simpson, J.T., Loman, N.J., and Loose, M. (2019). Reply
732 to ‘Errors in long-read assemblies can critically affect protein prediction.’ *Nat Biotechnol* 37,
733 127–128. 10.1038/s41587-018-0005-y.
- 734 17. Yassin, A. (2013). Phylogenetic classification of the Drosophilidae Rondani (Diptera):
735 the role of morphology in the postgenomic era. *Systematic Entomology* 38, 349–364.
- 736 18. Rondani, C. (1856). *Dipterologiae Italicae prodromus: Genera Italica Ordinis*
737 *Dipterorum* (Stocchi).
- 738 19. Egger, S. (1853). *Himmlische Waffenrüstung für die Jugend bestehend aus den*
739 *heiligen Sakramenten der Busse, des Altars und der Firmung: Ein praktischer Unterricht*
740 (Schmid).
- 741 20. Throckmorton, L. (1975). The phylogeny, ecology, and geography of *Drosophila*. In.
- 742 21. Keiper, J.B., Walton, W.E., and Foote, B.A. (2002). Biology and ecology of higher
743 Diptera from freshwater wetlands. *Annu. Rev. Entomol.* 47, 207–232.
744 10.1146/annurev.ento.47.091201.145159.
- 745 22. Pollock, J.N. (2002). Observations on the biology and anatomy of Curtonotidae
746 (Diptera: Schizophora). *Journal of Natural History* 36, 1725–1745.
747 10.1080/00222930110061869.
- 748 23. Markow, T.A., and O’Grady, P.M. (2005). Evolutionary genetics of reproductive
749 behavior in *Drosophila*: connecting the dots. *Annu. Rev. Genet.* 39, 263–291.
750 10.1146/annurev.genet.39.073003.112454.
- 751 24. Ashburner, M. (1981). Entomophagous and other bizarre *Drosophilidae*. In.
- 752 25. Duchêne, D., Duchêne, S., and Ho, S.Y.W. (2014). Tree imbalance causes a bias in
753 phylogenetic estimation of evolutionary timescales using heterochronous sequences.
754 *Molecular Ecology Resources* 15, 785–794. 10.1111/1755-0998.12352.

- 755 26. Shell, W.A., Steffen, M.A., Pare, H.K., Seetharam, A.S., Severin, A.J., Toth, A.L., and
756 Rehan, S.M. (2021). Sociality sculpts similar patterns of molecular evolution in two
757 independently evolved lineages of eusocial bees. *Commun Biol* 4, 253. 10.1038/s42003-021-
758 01770-6.
- 759 27. Noll, F.B. (2002). Behavioral phylogeny of corbiculate Apidae (Hymenoptera;
760 Apinae), with special reference to social behavior. *Cladistics* 18, 137–153. 10.1111/j.1096-
761 0031.2002.tb00146.x.
- 762 28. Galang, K.C., Croft, J.R., Thompson, G.J., and Percival-Smith, A. (2019). Analysis of
763 the *Drosophila melanogaster* anti-ovarian response to honey bee queen mandibular
764 pheromone. *Insect Molecular Biology* 28, 99–111. 10.1111/imb.12531.
- 765 29. Grimaldi, D., and Underwood, B.A. (1986). *Megabraula*, a new genus for two new
766 species of Braulidae (Diptera), and a discussion of braulid evolution. *System Entomol* 11,
767 427–438. 10.1111/j.1365-3113.1986.tb00534.x.
- 768 30. Dobson, J.R. (1999). A “bee-louse” *Braula schmitzi* örösi-pál (Diptera: Braulidae)
769 new to the British Isles, and the status of *Braula* spp. in England and Wales.
- 770 31. Kelley, J.L., Peyton, J.T., Fiston-Lavier, A.-S., Teets, N.M., Yee, M.-C., Johnston,
771 J.S., Bustamante, C.D., Lee, R.E., and Denlinger, D.L. (2014). Compact genome of the
772 Antarctic midge is likely an adaptation to an extreme environment. *Nat Commun* 5, 4611.
773 10.1038/ncomms5611.
- 774 32. Kim, B.Y., Wang, J.R., Miller, D.E., Barmina, O., Delaney, E., Thompson, A.,
775 Comeault, A.A., Peede, D., D’Agostino, E.R., Pelaez, J., et al. (2021). Highly contiguous
776 assemblies of 101 drosophilid genomes. *eLife* 10, e66405. 10.7554/eLife.66405.
- 777 33. Cantarel, B.L., Korf, I., Robb, S.M.C., Parra, G., Ross, E., Moore, B., Holt, C.,
778 Alvarado, A.S., and Yandell, M. (2008). MAKER: An easy-to-use annotation pipeline
779 designed for emerging model organism genomes. *Genome Res.* 18, 188–196.
780 10.1101/gr.6743907.
- 781 34. Korf, I. (2004). Gene finding in novel genomes. *BMC Bioinformatics* 5, 59.
782 10.1186/1471-2105-5-59.
- 783 35. König, S., Romoth, L.W., Gerischer, L., and Stanke, M. (2016). Simultaneous gene
784 finding in multiple genomes. *Bioinformatics* 32, 3388–3395. 10.1093/bioinformatics/btw494.
- 785 36. van Breugel, F., and Dickinson, M.H. (2017). Superhydrophobic diving flies (*Ephydra*
786 *hians*) and the hypersaline waters of Mono Lake. *Proceedings of the National Academy of*
787 *Sciences* 114, 13483–13488. 10.1073/pnas.1714874114.
- 788 37. Flynn, J.M., Hubley, R., Goubert, C., Rosen, J., Clark, A.G., Feschotte, C., and Smit,
789 A.F. (2020). RepeatModeler2 for automated genomic discovery of transposable element
790 families. *Proceedings of the National Academy of Sciences* 117, 9451–9457.
791 10.1073/pnas.1921046117.
- 792 38. Smit, A.F.A., Hubley, R., and Green, P. (2015). RepeatMasker Open-4.0. 2013–2015
793 <http://www.repeatmasker.org/>.
- 794 39. Mérel, V., Boulesteix, M., Fablet, M., and Vieira, C. (2020). Transposable elements in
795 *Drosophila*. *Mobile DNA* 11, 23. 10.1186/s13100-020-00213-z.
- 796 40. Gilbert, C., Peccoud, J., and Cordaux, R. (2021). Transposable elements and the
797 evolution of insects. *Annu. Rev. Entomol.* 66, 355–372. 10.1146/annurev-ento-070720-
798 074650.
- 799 41. Venner, S., Miele, V., Terzian, C., Biéumont, C., Daubin, V., Feschotte, C., and
800 Pontier, D. (2017). Ecological networks to unravel the routes to horizontal transposon
801 transfers. *PLOS Biology* 15, e2001536. 10.1371/journal.pbio.2001536.
- 802 42. Barry, E.G., Witherspoon, D.J., and Lampe, D.J. (2004). A Bacterial Genetic Screen
803 Identifies Functional Coding Sequences of the Insect *mariner* Transposable Element *Famar1*
804 Amplified From the Genome of the Earwig, *Forficula auricularia*. *Genetics* 166, 823–833.

805 10.1534/genetics.166.2.823.

806 43. Carr, S.M. (2023). Multiple mitogenomes indicate things fall apart with Out of Africa
807 or Asia hypotheses for the phylogeographic evolution of honey bees (*Apis mellifera*). *Sci Rep*
808 *13*, 9386. 10.1038/s41598-023-35937-4.

809 44. Gilbert, C., Schaack, S., Pace II, J.K., Brindley, P.J., and Feschotte, C. (2010). A role
810 for host–parasite interactions in the horizontal transfer of transposons across phyla. *Nature*
811 *464*, 1347–1350. 10.1038/nature08939.

812 45. Gilbert, C., and Maumus, F. (2022). Multiple Horizontal Acquisitions of Plant Genes
813 in the Whitefly *Bemisia tabaci*. *Genome Biology and Evolution* *14*, evac141.
814 10.1093/gbe/evac141.

815 46. Emms, D.M., and Kelly, S. (2019). OrthoFinder: phylogenetic orthology inference for
816 comparative genomics. *Genome Biol* *20*, 1–14. 10.1186/s13059-019-1832-y.

817 47. Mendes, F.K., Vanderpool, D., Fulton, B., and Hahn, M.W. (2020). CAFE 5 models
818 variation in evolutionary rates among gene families. *Bioinformatics* *36*, 5516–5518.
819 10.1093/bioinformatics/btaa1022.

820 48. Thurmond, J., Goodman, J.L., Strelets, V.B., Attrill, H., Gramates, L.S., Marygold,
821 S.J., Matthews, B.B., Millburn, G., Antonazzo, G., Trovisco, V., et al. (2019). FlyBase 2.0:
822 the next generation. *Nucleic Acids Research* *47*, D759–D765. 10.1093/nar/gky1003.

823 49. Evans, J.D., Aronstein, K., Chen, Y.P., and Hetru, C. (2006). Immune pathways and
824 defence mechanisms in honey bees *Apis mellifera*. *Insect Molecular Biology*.

825 50. Berenbaum, M.R., and Johnson, R.M. (2015). Xenobiotic detoxification pathways in
826 honey bees. *Current Opinion in Insect Science* *10*, 51–58. 10.1016/j.cois.2015.03.005.

827 51. Chan, Q.W.T., Chan, M.Y., Logan, M., Fang, Y., Higo, H., and Foster, L.J. (2013).
828 Honey bee protein atlas at organ-level resolution. *Genome Res.* *23*, 1951–1960.
829 10.1101/gr.155994.113.

830 52. Winston, M.L. (1987). *The Biology of the Honey Bee* (Harvard University Press).

831 53. Weiss, L.A., Dahanukar, A., Kwon, J.Y., Banerjee, D., and Carlson, J.R. (2011). The
832 Molecular and Cellular Basis of Bitter Taste in *Drosophila*. *Neuron* *69*, 258–272.
833 10.1016/j.neuron.2011.01.001.

834 54. Karpe, S.D., Tiwari, V., and Ramanathan, S. (2021). InsectOR—Webserver for
835 sensitive identification of insect olfactory receptor genes from non-model genomes. *PLoS*
836 *ONE* *16*, e0245324. 10.1371/journal.pone.0245324.

837 55. Sadd, B.M., Barribeau, S.M., Bloch, G., de Graaf, D.C., Dearden, P., Elsik, C.G.,
838 Gadau, J., Grimmelikhuijzen, C.J., Hasselmann, M., Lozier, J.D., et al. (2015). The genomes
839 of two key bumblebee species with primitive eusocial organization. *Genome Biol* *16*, 1–32.
840 10.1186/s13059-015-0623-3.

841 56. Robertson, H.M., and Wanner, K.W. (2006). The chemoreceptor superfamily in the
842 honey bee, *Apis mellifera*: expansion of the odorant, but not gustatory, receptor family.
843 *Genome Res.* *16*, 1395–1403. 10.1101/gr.5057506.

844 57. Ni, L. (2021). The structure and function of ionotropic receptors in *Drosophila*. *Front.*
845 *Mol. Neurosci.* *13*, 638839. 10.3389/fnmol.2020.638839.

846 58. Park, D., Jung, J.W., Choi, B.-S., Jayakodi, M., Lee, J., Lim, J., Yu, Y., Choi, Y.-S.,
847 Lee, M.-L., Park, Y., et al. (2015). Uncovering the novel characteristics of Asian honey bee,
848 *Apis cerana*, by whole genome sequencing. *BMC Genomics* *16*, 1. 10.1186/1471-2164-16-1.

849 59. Karpe, S.D., Jain, R., Brockmann, A., and Sowdhamini, R. (2016). Identification of
850 Complete Repertoire of *Apis florea* Odorant Receptors Reveals Complex Orthologous
851 Relationships with *Apis mellifera*. *Genome Biology and Evolution* *8*, 2879–2895.
852 10.1093/gbe/evw202.

853 60. Münch, D., and Galizia, C.G. (2016). DoOR 2.0 - Comprehensive mapping of
854 *Drosophila melanogaster* odorant responses. *Sci Rep* *6*, 21841. 10.1038/srep21841.

- 855 61. Wang, Z., and Tan, K. (2019). Honey Bee Alarm Pheromone Mediates
856 Communication in Plant–Pollinator–Predator Interactions. *Insects* *10*, 366.
857 10.3390/insects10100366.
- 858 62. Machado, A.M., Miguel, M.G., Vilas-Boas, M., and Figueiredo, A.C. (2020). Honey
859 Volatiles as a Fingerprint for Botanical Origin—A Review on their Occurrence on Monofloral
860 Honey. *Molecules* *25*, 374. 10.3390/molecules25020374.
- 861 63. Starowicz, M., Hanus, P., Lamparski, G., and Sawicki, T. (2021). Characterizing the
862 Volatile and Sensory Profiles, and Sugar Content of Beeswax, Beebread, Bee Pollen, and
863 Honey. *Molecules* *26*, 3410. 10.3390/molecules26113410.
- 864 64. Noël, A., Dumas, C., Rottier, E., Beslay, D., Costagliola, G., Ginies, C., Nicolè, F.,
865 Rau, A., Conte, Y.L., and Mondet, F. (2023). Detailed chemical analysis of honey bee (*Apis*
866 *mellifera*) worker brood volatile profile from egg to emergence. *PLOS ONE* *18*, e0282120.
867 10.1371/journal.pone.0282120.
- 868 65. Collins, A.M., and Blum, M.S. (1983). Alarm responses caused by newly identified
869 compounds derived from the honeybee sting. *J Chem Ecol* *9*, 57–65. 10.1007/BF00987770.
- 870 66. Torto, B., Boucias, D.G., Arbogast, R.T., Tumlinson, J.H., and Teal, P.E.A. (2007).
871 Multitrophic interaction facilitates parasite–host relationship between an invasive beetle and
872 the honey bee. *Proceedings of the National Academy of Sciences* *104*, 8374–8378.
873 10.1073/pnas.0702813104.
- 874 67. Van Oystaeyen, A., Oliveira, R.C., Holman, L., van Zweden, J.S., Romero, C., Oi,
875 C.A., d’Ettorre, P., Khalesi, M., Billen, J., Wäckers, F., et al. (2014). Conserved Class of
876 Queen Pheromones Stops Social Insect Workers from Reproducing. *Science* *343*, 287–290.
877 10.1126/science.1244899.
- 878 68. Camiletti, A.L., Percival-Smith, A., Croft, J.R., and Thompson, G.J. (2016). A novel
879 screen for genes associated with pheromone-induced sterility. *Sci Rep* *6*, 36041.
880 10.1038/srep36041.
- 881 69. Stensmyr, M.C., Dweck, H.K.M., Farhan, A., Ibba, I., Strutz, A., Mukunda, L., Linz,
882 J., Grabe, V., Steck, K., Lavista-Llanos, S., et al. (2012). A Conserved Dedicated Olfactory
883 Circuit for Detecting Harmful Microbes in *Drosophila*. *Cell* *151*, 1345–1357.
884 10.1016/j.cell.2012.09.046.
- 885 70. Senthilan, P.R., and Helfrich-Förster, C. (2016). Rhodopsin 7—The unusual Rhodopsin
886 in *Drosophila*. *PeerJ* *4*, e2427. 10.7717/peerj.2427.
- 887 71. Zanini, D., Giraldo, D., Warren, B., Katana, R., Andrés, M., Reddy, S., Pauls, S.,
888 Schwedhelm-Domeyer, N., Geurten, B.R.H., and Göpfert, M.C. (2018). Proprioceptive Opsin
889 Functions in *Drosophila* Larval Locomotion. *Neuron* *98*, 67–74.e4.
890 10.1016/j.neuron.2018.02.028.
- 891 72. Leung, N.Y., and Montell, C. (2017). Unconventional Roles of Opsins. *Annu. Rev.*
892 *Cell Dev. Biol.* *33*, 241–264. 10.1146/annurev-cellbio-100616-060432.
- 893 73. Mishra, A.K., Fritsch, C., Voutev, R., Mann, R.S., and Sprecher, S.G. (2021).
894 Homothorax controls a binary Rhodopsin switch in *Drosophila* ocelli. *PLOS Genetics* *17*,
895 e1009460. 10.1371/journal.pgen.1009460.
- 896 74. Partha, R., Chauhan, B.K., Ferreira, Z., Robinson, J.D., Lathrop, K., Nischal, K.K.,
897 Chikina, M., and Clark, N.L. (2017). Subterranean mammals show convergent regression in
898 ocular genes and enhancers, along with adaptation to tunneling. *eLife* *6*, e25884.
899 10.7554/eLife.25884.
- 900 75. Policarpo, M., Fumey, J., Lafargeas, P., Naquin, D., Thermes, C., Naville, M.,
901 Dechaud, C., Volff, J.-N., Cabau, C., Klopp, C., et al. (2021). Contrasting Gene Decay in
902 Subterranean Vertebrates: Insights from Cavefishes and Fossorial Mammals. *Molecular*
903 *Biology and Evolution* *38*, 589–605. 10.1093/molbev/msaa249.
- 904 76. Büscher, T.H., Petersen, D.S., Bijma, N.N., Bäumlner, F., Pirk, C.W.W., Büsse, S.,

905 Heepe, L., and Gorb, S.N. (2022). The exceptional attachment ability of the ectoparasitic bee
906 louse *Braula coeca* (Diptera, Braulidae) on the honeybee. *Physiological Entomology* *47*, 83–
907 95. 10.1111/phen.12378.

908 77. Roff, D.A. (1990). The Evolution of Flightlessness in Insects. *Ecological Monographs*
909 *60*, 389–421. 10.2307/1943013.

910 78. Miller, D.E., Staber, C., Zeitlinger, J., and Hawley, R.S. (2018). Highly Contiguous
911 Genome Assemblies of 15 *Drosophila* Species Generated Using Nanopore Sequencing. *G3:*
912 *Genes, Genomes, Genetics* *8*, 3131–3141. 10.1534/g3.118.200160.

913 79. Lu, H., Giordano, F., and Ning, Z. (2016). Oxford Nanopore MinION Sequencing and
914 Genome Assembly. *Genomics, Proteomics & Bioinformatics* *14*, 265–279.
915 10.1016/j.gpb.2016.05.004.

916 80. Leger, A., and Leonardi, T. (2019). pycoQC, interactive quality control for Oxford
917 Nanopore Sequencing. *JOSS* *4*, 1236. 10.21105/joss.01236.

918 81. Zimin, A.V., Puiu, D., Luo, M.-C., Zhu, T., Koren, S., Marçais, G., Yorke, J.A.,
919 Dvořák, J., and Salzberg, S.L. (2017). Hybrid assembly of the large and highly repetitive
920 genome of *Aegilops tauschii*, a progenitor of bread wheat, with the MaSuRCA mega-reads
921 algorithm. *Genome Res.* *27*, 787–792. 10.1101/gr.213405.116.

922 82. Kokot, M., Długosz, M., and Deorowicz, S. (2017). KMC 3: counting and
923 manipulating k-mer statistics. *Bioinformatics* *33*, 2759–2761. 10.1093/bioinformatics/btx304.

924 83. Ranallo-Benavidez, T.R., Jaron, K.S., and Schatz, M.C. (2020). GenomeScope 2.0 and
925 Smudgeplot for reference-free profiling of polyploid genomes. *Nat Commun* *11*, 1432.
926 10.1038/s41467-020-14998-3.

927 84. Laetsch, D.R., and Blaxter, M.L. (2017). BlobTools: Interrogation of genome
928 assemblies. Preprint at F1000Research, 10.12688/f1000research.12232.1
929 10.12688/f1000research.12232.1.

930 85. Buchfink, B., Xie, C., and Huson, D.H. (2015). Fast and sensitive protein alignment
931 using DIAMOND. *Nat Methods* *12*, 59–60. 10.1038/nmeth.3176.

932 86. Li, H. (2018). Minimap2: pairwise alignment for nucleotide sequences. *Bioinformatics*
933 *34*, 3094–3100. 10.1093/bioinformatics/bty191.

934 87. Muller, H., Ogereau, D., Da Lage, J.-L., Capdevielle, C., Pollet, N., Fortuna, T.,
935 Jeannette, R., Kaiser, L., and Gilbert, C. (2021). Draft nuclear genome and complete
936 mitogenome of the Mediterranean corn borer, *Sesamia nonagrioides*, a major pest of maize.
937 *G3 Genes|Genomes|Genetics* *11*, jkab155. 10.1093/g3journal/jkab155.

938 88. Camacho, C., Coulouris, G., Avagyan, V., Ma, N., Papadopoulos, J., Bealer, K., and
939 Madden, T.L. (2009). BLAST+: architecture and applications. *BMC Bioinformatics* *10*, 421.
940 10.1186/1471-2105-10-421.

941 89. Grabherr, M.G., Haas, B.J., Yassour, M., Levin, J.Z., Thompson, D.A., Amit, I.,
942 Adiconis, X., Fan, L., Raychowdhury, R., Zeng, Q., et al. (2011). Trinity: reconstructing a
943 full-length transcriptome without a genome from RNA-Seq data. *Nat Biotechnol* *29*, 644–652.
944 10.1038/nbt.1883.

945 90. Boekel, J., Chilton, J.M., Cooke, I.R., Horvatovich, P.L., Jagtap, P.D., Käll, L., Lehtiö,
946 J., Lukasse, P., Moerland, P.D., and Griffin, T.J. (2015). Multi-omic data analysis using
947 Galaxy. *Nat Biotechnol* *33*, 137–139. 10.1038/nbt.3134.

948 91. Hiltemann, S., Rasche, H., Gladman, S., Hotz, H.-R., Larivière, D., Blankenberg, D.,
949 Jagtap, P.D., Wollmann, T., Bretaudeau, A., Goué, N., et al. (2023). Galaxy Training: A
950 powerful framework for teaching! *PLOS Computational Biology* *19*, e1010752.
951 10.1371/journal.pcbi.1010752.

952 92. Katoh, K., and Standley, D.M. (2013). MAFFT multiple sequence alignment software
953 version 7: improvements in performance and usability. *Molecular Biology and Evolution* *30*,
954 772–780. 10.1093/molbev/mst010.

- 955 93. Minh, B.Q., Schmidt, H.A., Chernomor, O., Schrempf, D., Woodhams, M.D., von
956 Haeseler, A., and Lanfear, R. (2020). IQ-TREE 2: New Models and Efficient Methods for
957 Phylogenetic Inference in the Genomic Era. *Molecular Biology and Evolution* 37, 1530–1534.
958 10.1093/molbev/msaa015.
- 959 94. Hoang, D.T., Chernomor, O., von Haeseler, A., Minh, B.Q., and Vinh, L.S. (2018).
960 UFBoot2: improving the ultrafast bootstrap approximation. *Molecular Biology and Evolution*
961 35, 518–522. 10.1093/molbev/msx281.
- 962 95. Kalyaanamoorthy, S., Minh, B.Q., Wong, T.K.F., von Haeseler, A., and Jermini, L.S.
963 (2017). ModelFinder: fast model selection for accurate phylogenetic estimates. *Nat Methods*
964 14, 587–589. 10.1038/nmeth.4285.
- 965 96. Okada, T. (1962). Bleeding sap preference of the *Drosophilid* flies. *Japanese journal of*
966 *applied entomology and zoology* 6, 216–229. 10.1303/jjaez.6.216.
- 967 97. Pagel, M., and Meade, A. Bayesian analysis of correlated evolution of discrete
968 characters by reversible-jump markov chain monte carlo.
- 969 98. Yang, Z. (2007). PAML 4: phylogenetic analysis by maximum likelihood. *Molecular*
970 *Biology and Evolution* 24, 1586–1591. 10.1093/molbev/msm088.
- 971 99. Misof, B., Liu, S., Meusemann, K., Peters, R.S., Donath, A., Mayer, C., Frandsen,
972 P.B., Ware, J., Flouri, T., Beutel, R.G., et al. (2014). Phylogenomics resolves the timing and
973 pattern of insect evolution. *Science* 346, 763–767. 10.1126/science.1257570.
- 974 100. Suvorov, A., Kim, B.Y., Wang, J., Armstrong, E.E., Peede, D., D’Agostino, E.R.R.,
975 Price, D.K., Waddell, P.J., Lang, M., Courtier-Orgogozo, V., et al. (2022). Widespread
976 introgression across a phylogeny of 155 *Drosophila* genomes. *Current Biology* 32, 111-
977 123.e5. 10.1016/j.cub.2021.10.052.
- 978 101. Revell, L.J. (2012). phytools: an R package for phylogenetic comparative biology (and
979 other things). *Methods in Ecology and Evolution* 3, 217–223. 10.1111/j.2041-
980 210X.2011.00169.x.
- 981 102. Rognes, T., Flouri, T., Nichols, B., Quince, C., and Mahé, F. (2016). VSEARCH: a
982 versatile open source tool for metagenomics. *PeerJ* 4, e2584. 10.7717/peerj.2584.
- 983 103. Lampe, D.J., Witherspoon, D.J., Soto-Adames, F.N., and Robertson, H.M. (2003).
984 Recent horizontal transfer of mellifera subfamily mariner transposons into insect lineages
985 representing four different orders shows that selection acts only during horizontal transfer.
986 *Mol Biol Evol* 20, 554–562. 10.1093/molbev/msg069.
- 987 104. Zhang, H.-H., Peccoud, J., Xu, M.-R.-X., Zhang, X.-G., and Gilbert, C. (2020).
988 Horizontal transfer and evolution of transposable elements in vertebrates. *Nat Commun* 11,
989 1362. 10.1038/s41467-020-15149-4.
- 990 105. Edgar, R.C. (2004). MUSCLE: a multiple sequence alignment method with reduced
991 time and space complexity. *BMC Bioinformatics* 5, 113. 10.1186/1471-2105-5-113.
- 992 106. Gilleland, E., and Katz, R.W. (2016). extRemes 2.0: An Extreme Value Analysis
993 Package in R. *Journal of Statistical Software* 72, 1–39. 10.18637/jss.v072.i08.
- 994 107. Slater, G.S.C., and Birney, E. (2005). Automated generation of heuristics for
995 biological sequence comparison. *BMC Bioinformatics* 6, 31. 10.1186/1471-2105-6-31.
- 996 108. Murray, M.H., and Blume, J.D. (2021). FDRestimation: Flexible False Discovery Rate
997 Computation in R. *F1000Res* 10, 441. 10.12688/f1000research.52999.2.
- 998 109. Montell, C. (2009). A taste of the *Drosophila* gustatory receptors. *Current Opinion in*
999 *Neurobiology* 19, 345–353. 10.1016/j.conb.2009.07.001.

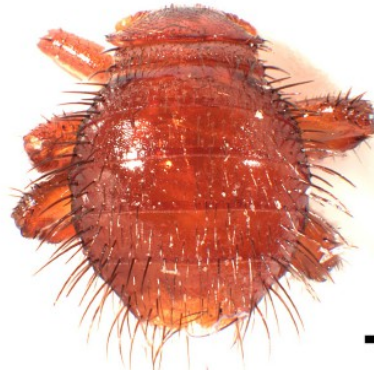
1000

Figure 1

A



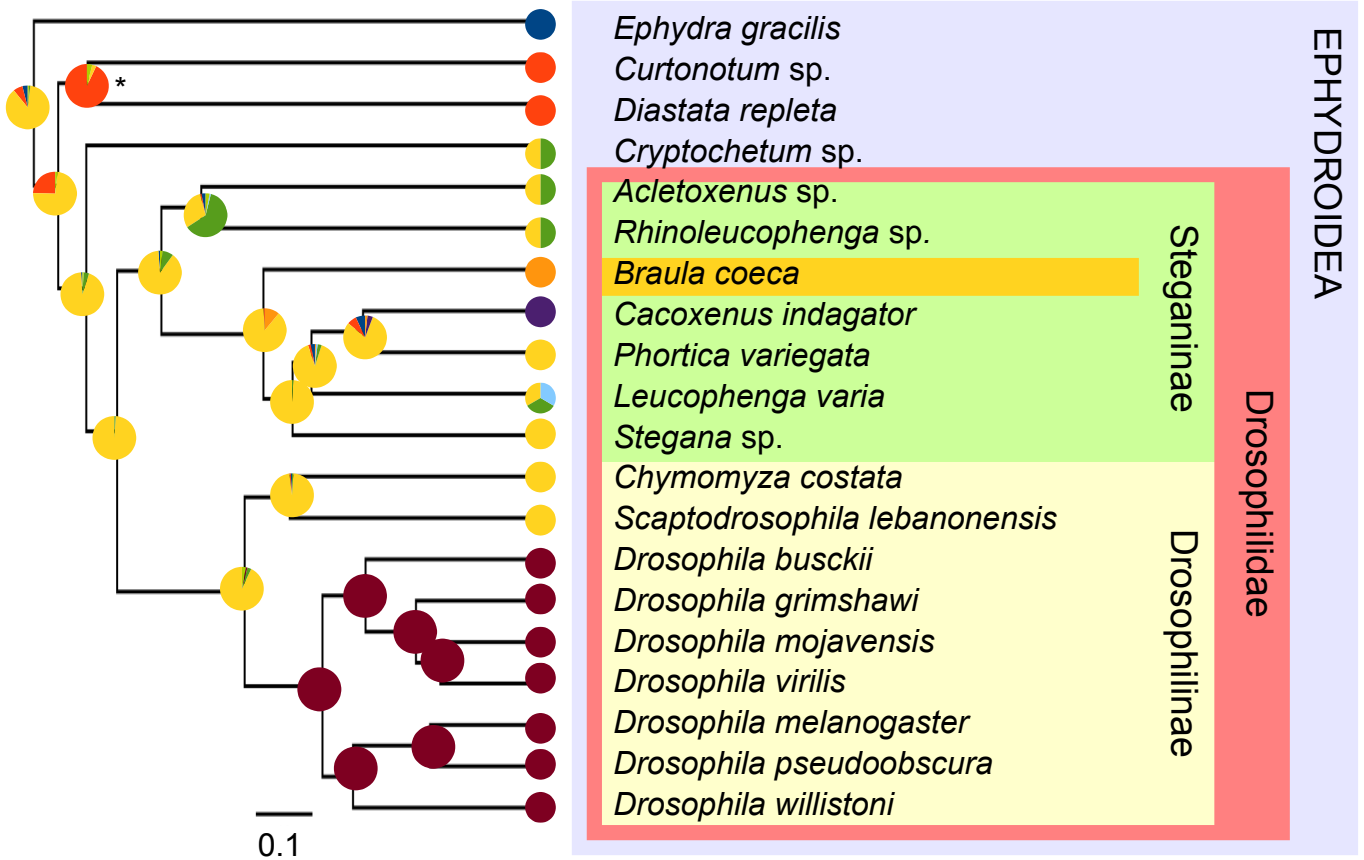
B



C



D



Predominant niche

- Algae + marsh plants
- Dung

- Plant sap
- Scale insects

- Fruits
- Fungi
- Solitary bee inquilinism
- Social bee inquilinism

Figure 2

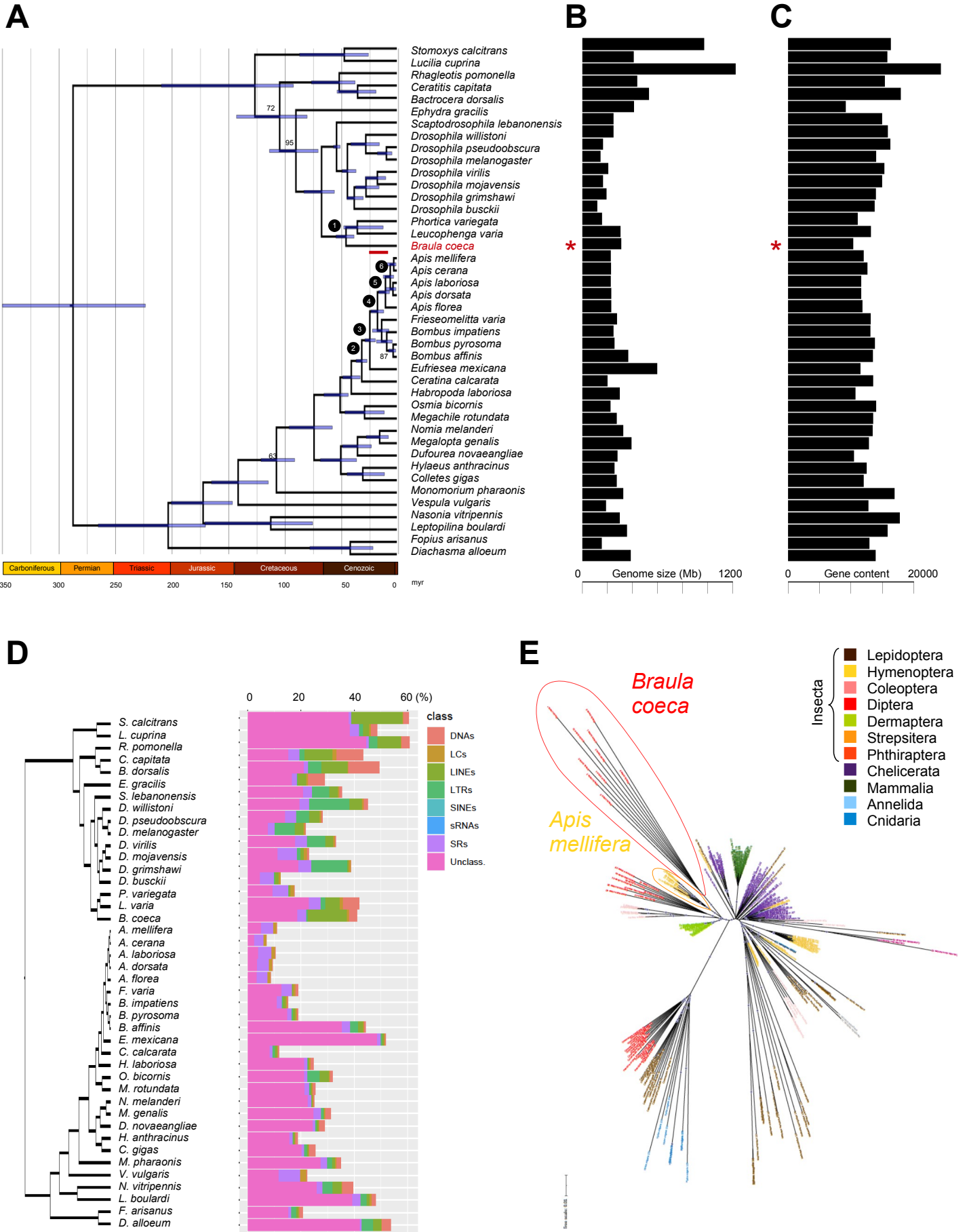


Table 1 – Rapidly evolving gene groups in *Braula coeca* show parallel reduction with bees. See also Figure S3. Gene groups were defined according to *D. melanogaster* genes clustered with orthologous sequences from 42 dipteran and hymenopteran genomes by OrthoFinder. Putative functions of each group are given following FlyBase definitions and references therein. Evolutionary rate was estimated by CAFE5, with *p*-values corrected for multiple testing using False Discovery Rate (FDR) analysis.

Gene group	Function	Evolution in <i>Braula</i>		Evolution in bees
		Change	FDR <i>p</i> -value	
GUSTATORY RECEPTORS	Chemosensory	Reduced	1.7×10^{-4}	Reduced in bees
DIVERGENT IONOTROPIC RECEPTORS	Chemosensory	Reduced	1.7×10^{-4}	Reduced in Hymenoptera
S1A NON-PEPTIDASE HOMOLOGS	Immunity, morphogenesis	Reduced	1.9×10^{-4}	Reduced in bees (particularly in <i>A. mellifera</i>)
CYTOCHROME P450 - CYP3 CLAN	Detoxification	Reduced	9.8×10^{-4}	Reduced in <i>Apis</i> (particularly in <i>A. mellifera</i>)
ODORANT RECEPTORS	Chemosensory	Reduced	9.9×10^{-4}	Reduced in the Apidae
ODORANT BINDING PROTEINS	Chemosensory	Reduced	0.0012	Reduced in bees
CYTOSOLIC GLUTATHIONE S-TRANSFERASES	Detoxification	Reduced	0.0034	Reduced in <i>Apis</i>
ECDYSTEROID KINASE-LIKE	Detoxification	Reduced	0.0034	Reduced in bees
C-TYPE LECTIN-LIKE	Immunity	Reduced	0.0072	Reduced in Hymenoptera
SLC22 FAMILY OF ORGANIC IONS TRANSPORTERS	Development, detoxification	Reduced	0.0084	Reduced in <i>Apis</i>
SLC2 FAMILY OF HEXOSE SUGAR TRANSPORTERS	Metabolism	Reduced	0.0144	
S1A SERINE PROTEASES - CHYMOTRYPSIN-LIKE	Metabolism, immunity, morphogenesis	Reduced	0.0144	Reduced in bees
CHITIN BINDING DOMAIN-CONTAINING PROTEINS	Morphogenesis, immunity	Reduced	0.0233	Reduced in bees
CARBOXYLESTERASES	Detoxification	Reduced	0.0450	Reduced in longue-tongued bees (but not in <i>A. mellifera</i>)
S1A SERINE PROTEASES - TRYPSIN-LIKE	Metabolism, immunity, morphogenesis	Reduced	0.0450	Reduced in bees
CYTOCHROME P450 - CYP4 CLAN	Detoxification	Reduced	0.0478	Reduced in bees
DORSAL GROUP	Morphogenesis, immunity	Reduced	0.0478	Reduced in Hymenoptera

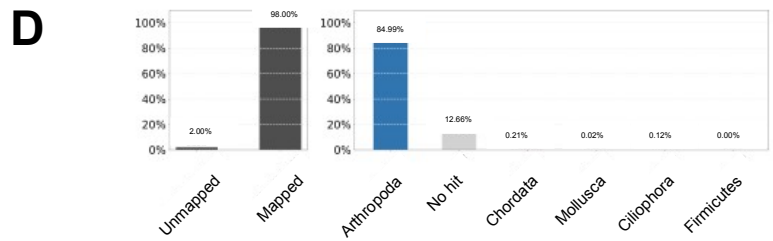
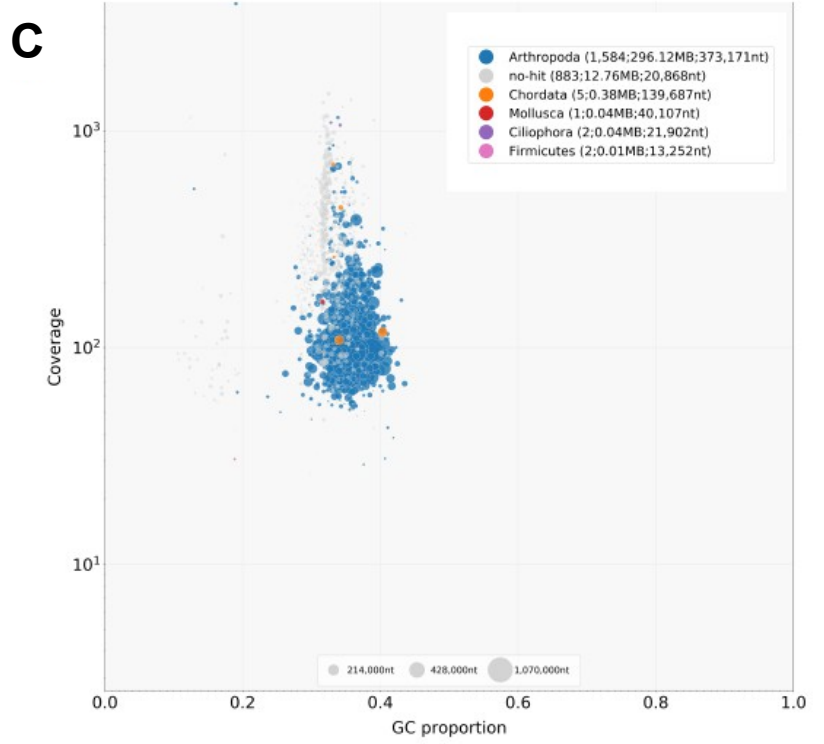
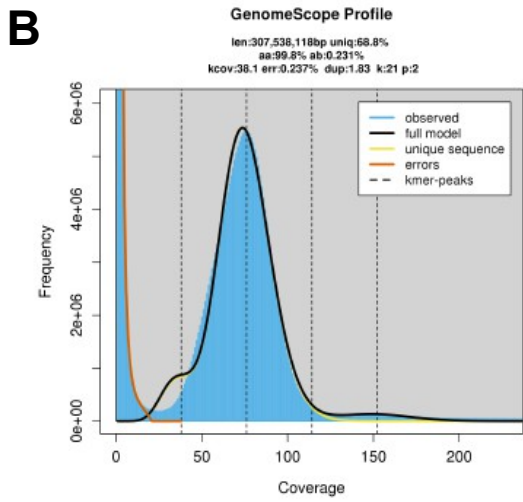
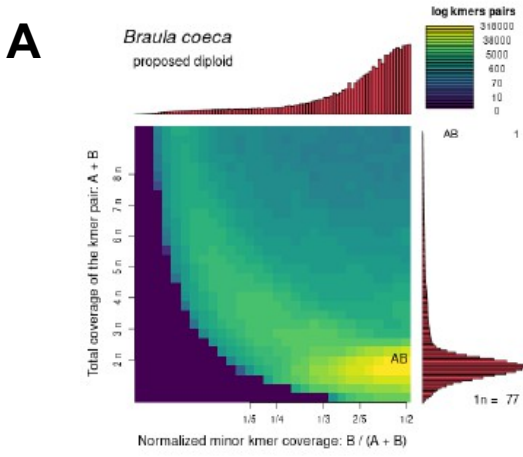


Figure S1. Features of *Braula coeca* genome assembly, Related to STAR Methods.

(A) Smudgeplot comparing the sum of heterozygous kmer pair coverages (A+B) to their relative coverage of the minor kmer (B/A+B). The hottest smudge corresponds to expected diploid kmer pairs (AB).

(B) Kmer profile spectrum estimating the length of the genome at 307,538,118 bp generated by GenomeScope2.

(C) Square-binned blob plot showing the distribution of assembly scaffolds on GC proportion and coverage axes. Squares within each bin are colored according to taxonomic annotation and scaled according to total span.

(D) ReadCovPlots generated by Blobtools visualising the proportion of reads of *B. coeca* that are unmapped or mapped and showing the percentage of mapped reads by taxonomic group, as barcharts.

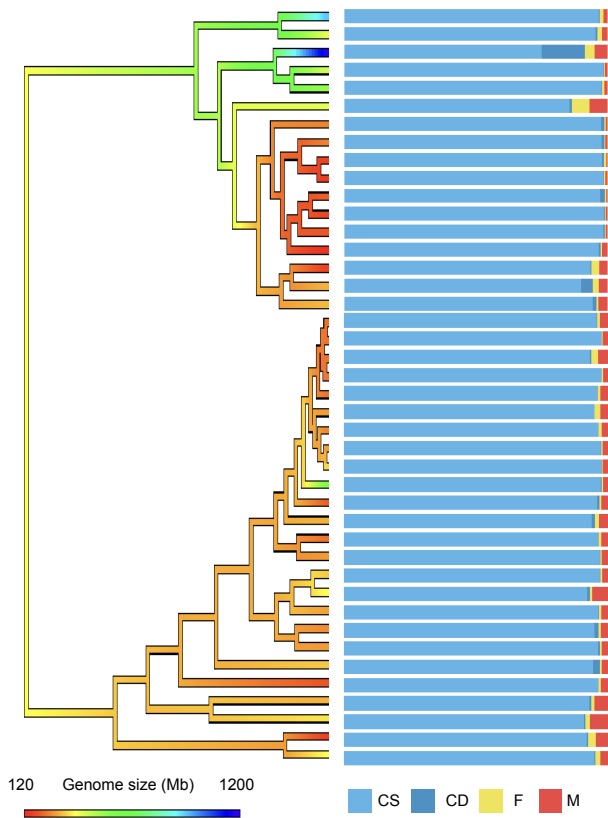
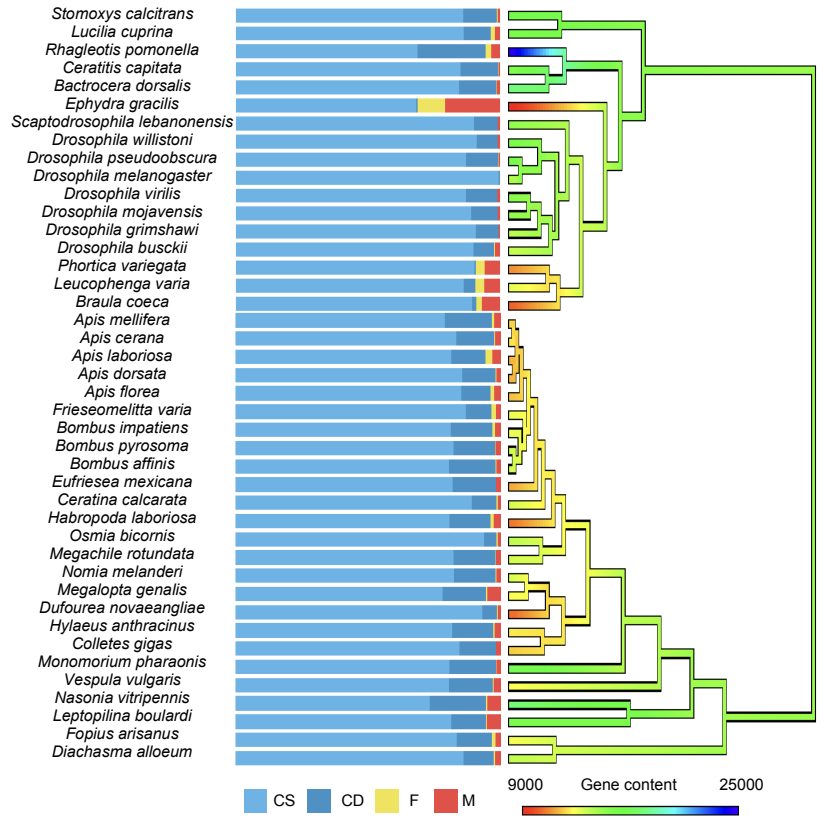
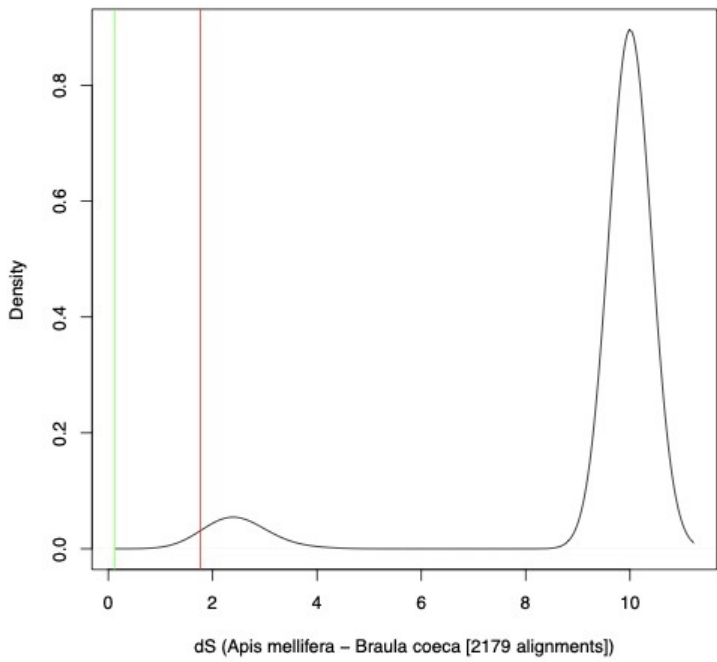
A**B****C**

Figure S2. Genome size, gene content and completeness of assembly and annotation of 42 dipteran and hymenopteran genomes and evidence for a horizontal transposon transfer between *B. coeca* and *A. mellifera*, Related to Figure 2.

(A) Genome-size evolution and genome assembly completeness inferred by BUSCO across 42 dipteran and hymenopteran species.

(B) Gene content evolution and genome annotation completeness inferred by BUSCO across 42 dipteran and hymenopteran species.

Branch colors in A and B reflect inferred ancestral reconstructions using fastanc in phytools. CS = complete and single-copy BUSCOs; CD = complete and duplicated BUSCOs; F = fragmented BUSCOs; M = missing BUSCOs.

(C) Horizontal transposon transfer between *Braula coeca* and *Apis mellifera*.

Comparison of Famar1-like transposon synonymous distance (dS) and orthologous gene synonymous distances between *Braula coeca* and *Apis mellifera*. The red line indicates the 0.5% quantile (=1.76) of the distribution of orthologous gene dS calculated over 2,179 codon alignments. The distribution is bimodal, with genes having highly saturated dS values showing a peak centered on 9.99 and highly conserved genes showing less saturated dS values showing another peak around 2.5. The *Famar1*-like dS (green line, = 0.12) was calculated over the transposase open reading frame of one copy of the element extracted from the *A. mellifera* genome and another copy from the *B. coeca* genome.

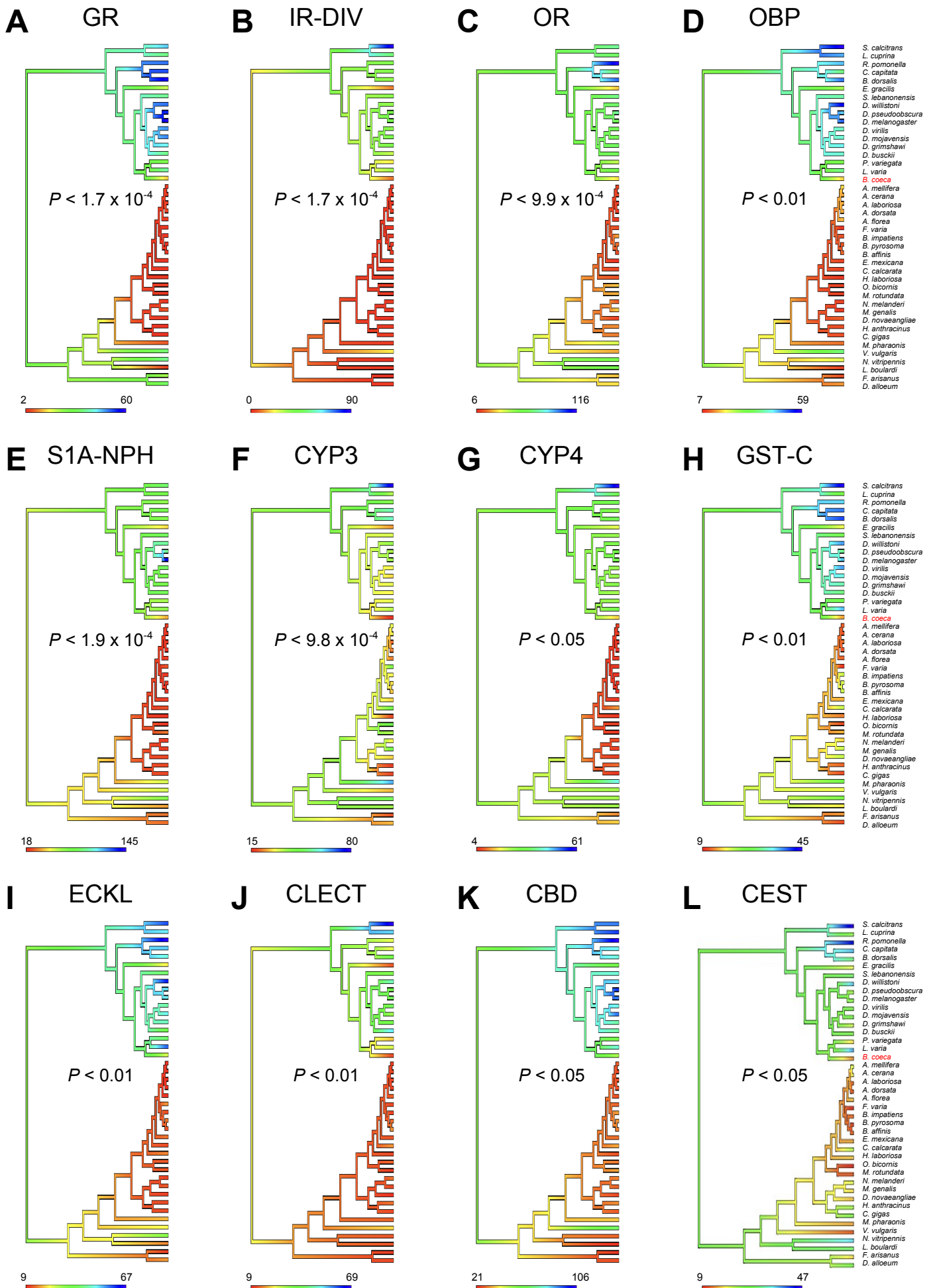


Figure S3. Ancestral gene count reconstructions of 12 gene groups significantly evolving in *Braula coeca* after correction for multiple testing, Related to Table 1. For each panel, the species tree from Figure 2 is given with branch colors reflecting inferred ancestral family size reconstruction using fastanc in phytools.

(A) GR = Gustatory Receptors

(B) IR-DIV = Divergent Ionotropic Receptors

(C) OR = Odorant Receptors

(D) OBP = Odorant Binding Proteins

(E) S1A-NPH = S1a Non-Peptidase Homologs

(F) CYP3 = Cytochrome P450 - CYP3 Clan

(G) CYP4 = Cytochrome P450 - CYP4 Clan

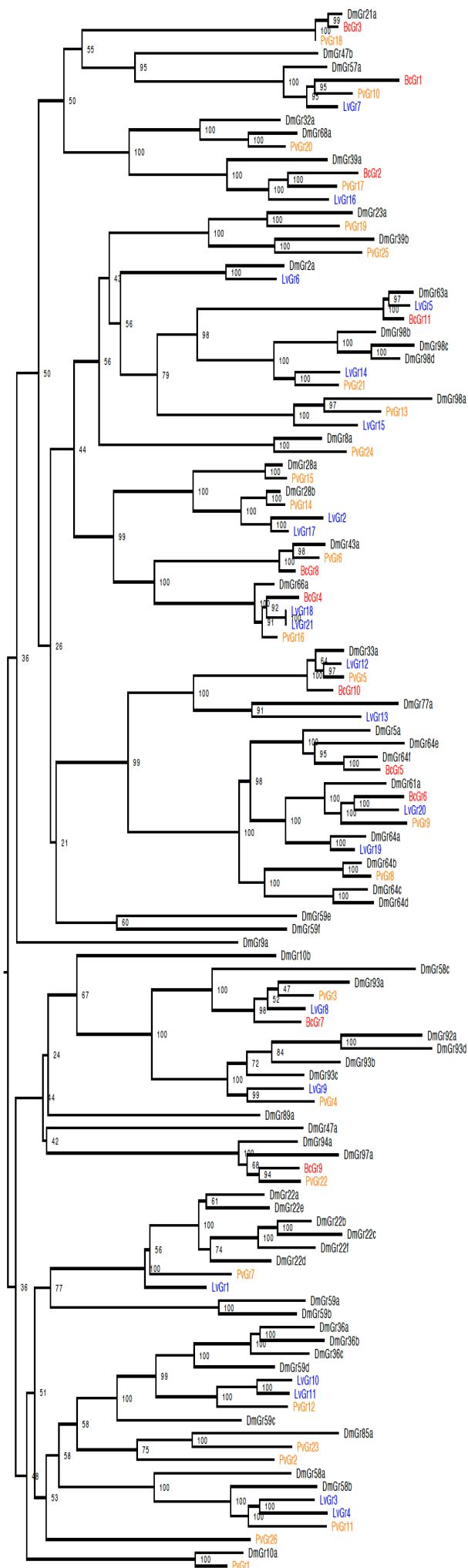
(H) GST-C = Cytosolic Glutathione S-Transferases

(I) ECKL = Ecdysteroid Kinase-Like

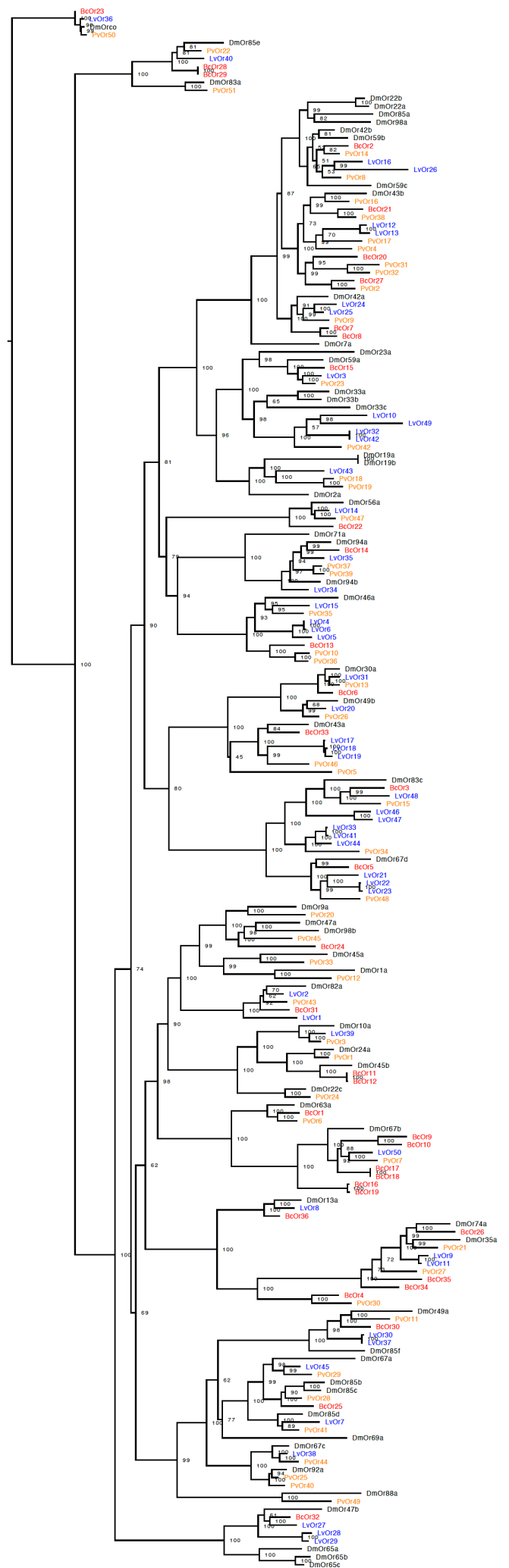
(J) CLECT = C-Type Lectin-Like

(K) CBD = Chitin Binding Domain-Containing Proteins

(L) CEST = Carboxylesterases

A

0.4

B

0.7

Figure S4. Maximum-likelihood phylogeny of gustatory receptors (GRs) and odorant receptors (ORs), Related to Figure 3.

(A) Maximum-likelihood phylogeny of GRs from *D. melanogaster*, *B. coeca*, *L. varia* and *P. variegata*.

(B) Maximum-likelihood phylogeny of ORs from *D. melanogaster*, *B. coeca*, *L. varia* and *P. variegata*.